Performance Evaluation of Doubly Selective Fading in FBMC with Higher Order QAM for 5G Wireless Communications and Beyond

Wesene Getachew Wordofa

A Thesis Submitted to the Department of Electronics and Communication Engineering

School of Electrical Engineering and Computing

Presented in Partial Fulfilment of the Requirement for the Degree of Master's in Electronics and Communication Engineering

Office of Graduate Studies

Adama Science and Technology University

June, 2024

Adama, Ethiopia

Performance Evaluation of Doubly Selective Fading in FBMC with Higher Order QAM for 5G Wireless Communications and Beyond

Wesene Getachew Wordofa

Major advisor: Dr. Demissie Jobir Gelmecha

Co-advisor: Dr. Selewendim Eshetu

A Thesis Submitted to the Department of Electronics and Communication Engineering

School of Electrical Engineering and Computing

Presented in Partial Fulfilment of the Requirement for the Degree of Master’s in Electronics and Communication Engineering

Office of Graduate Studies
Adama Science and Technology University

June, 2024

Adama, Ethiopia

DECLARATION

I declare that this thesis entitled **"*Performance Evaluation of Doubly Selective Fading in FBMC with Higher Order QAM for 5G Wireless Communications and Beyond*"** is my own work and has not been submitted to any university for similar purpose. The references used in this thesis are duly recognized by proper citations.

____________________________ __________________ __________________

Name of Student Signature Date

RECOMMENDATION OF ADVISORS

I, the major advisor of this thesis, hereby certify that I have closely advised the student while developing this thesis and read the draft thesis entitled **"*Performance Evaluation of Doubly Selective Fading in FBMC with Higher Order QAM for 5G Wireless Communications and beyond*"** prepared under our guidance by Wesene Getachew Wordofa. Therefore, I recommend the submission of the thesis to the department for further review and evaluation.

Dr. Demisse Jobir	___________________	_________________
Major Advisor	Signature	Date
Dr. Selewendim Eshetu	____________________	_________________
Co-advisor	Signature	Date

APPROVAL PAGE

We hereby certify that the recommendation and suggestion given by the thesis review committee are appropriately incorporated into the final thesis entitled **"*Performance Evaluation of Doubly Selective Fading in FBMC with Higher Order QAM for 5G Wireless Communications and beyond*"** prepared under our guidance by Wesene Getachew Wordofa. Therefore, we recommend the submission of this thesis to the department for further review and evaluation.

Dr. Demisse Jobir	____________________	______________
Major Advisor	Signature	Date
Dr. Selewendim Eshetu	______________	_________________
Co-advisor	Signature	Date

APPROVAL OF BOARD OF REVIEWERS

We, the undersigned, members of the Board of Reviewers of the thesis open defence by Wesene Getachew Wordofa have read and evaluated the thesis entitled **“*Performance Evaluation of Doubly Selective Fading in FBMC with Higher Order QAM for 5G Wireless Communications and Beyond*”** and assessed the understanding of the candidate about the proposed research. This is, therefore, to certify that the thesis is accepted and we recommend the implementation of the thesis.

______________________	______________	______________
Chairperson	Signature	Date
______________________	______________	______________
Reviewer 1	Signature	Date
______________________	______________	______________
Reviewer 2	Signature	Date

Final approval and acceptance of the thesis is contingent upon submission of its final copy to the Office of Postgraduate Studies (OPGS) through the Department Graduate Council (DGC) and School Graduate Committee (SGC).

______________________	______________	______________
Department Head	Signature	Date
______________________	______________	______________
School Dean	Signature	Date
______________________	______________	______________
Office of Postgraduate Studies, Dean	Signature	Date

TABLE OF CONTENTS

LIST OF FIGURES

LIST OF TABLES

LIST OF ABBREVIATIONS

AP	Auxiliary Pilot
BER	Bit-Error-Rate
CDP	Constructed Data Pilots
CFR	Channel Frequency Respond
CP	Cyclic Prefix
DFT	Discrete Fourier Transform
DNN	Deep Neural Network
FBMC	Filter bank multi-carrier
ICI	Inter-Carrier Interference
IEEE	Institute Of Electrical And Electronics Engineers
IFFT/FFT	Inverse Fast Fourier Transform/ Fast Fourier Transform
ISI	Inter Symbol Interference
LMMSE	Linear Minimum Mean Square
LS	Least Square
MIMO	Multiple-Input And Multiple-Output
MSE	Mean-Squared-Error
NOMA	Non Orthogonal Multiple Access
OFDM	Orthogonal Frequency Division Multiplexing
OMP	Orthogonal Matching Pursuit
OQAM	Orthogonal Quadrature Amplitude Modulation
PAPR	Peak-to-Average Power Ratio
ROMP	Regularized Orthogonal Matching Pursuit
SASP	Sparse Adaptive Subspace Pursuit
SER	Symbol Error Rate
SNR	Signal-Noise-Ratio
ST	Superimposed Training
STA	Spectral Temporal Averaging
UFMC	Universal Filter Multicarrier
WOLA-OFDM	Weighted Overlap and Added Orthogonal Frequency Division Multiplexing

ABSTRACT

Filter bank multi-carrier (FBMC) modulation has gained significant attention as a potential candidate for physical data communication in the fifth generation (5G) and beyond wireless networks. Wireless channels, characterized by high mobility and abundant scatters, are prone to time-selective fading and frequency-selective fading that has been known as a "doubly selective channel." Broadband transmission systems encounter formidable challenges in channel estimation and equalization within such channels. The presence of high mobility gives rise to inter-carrier interference (ICI), while multipath transmission introduces inter-symbol interference (ISI). This thesis compared the performance of different channel estimation techniques in FBMC. Moreover, Iterative interference cancellation scheme is considered to address interference issues at pilot and data positions. Additionally, a suboptimal Minimum Mean Square Error (MMSE) equalization method, guided by a threshold judgment based on the variability of interference power was presented. This method utilizes normalized interference power thresholds to estimate the ISI dimension, minimizing equalization data and effectively mitigating the impact of ISI for efficient equalization. This research significantly contributes to the evolution of channel estimation techniques in FBMC, ultimately bolstering the reliability and performance of data communication in 5G wireless networks. In this thesis the performance of FBMC high order QAM in doubly selective fading channel is investigated with various performance. According to this, FBMC showed a much higher efficiency of $\rho = 0.97$ providing data rate approximately 50 % higher than in f-OFDM. Based on that the performance of FBMC is always the best one but its performances is comparable with now very the UFMC ones by providing maximum capacity value is 3.5 higher than the OFDM one but it is only 5% higher than UFMC. It can be observed from the result that FBMC revealed high performance compared to other multicarrier modulation techniques.

Keywords: *Inter-carrier interference, Minimum mean square error, Channel estimation, Filter bank multi-carrier, Doubly selective fading.*

CHAPATER ONE

1. INTRODUCTION

1.1 Background of the Study

The transfer of data and voice over a wireless network occurs without the need for cables or wires. Data is sent by electromagnetic signals that are broadcast from sending facilities to intermediate and end-user devices in lieu of a physical link. Wireless communication technologies continue to evolve and advance, providing faster speeds, increased capacity, and improved reliability. They play a crucial role in shaping the digital age and connecting people and devices worldwide.

Multicarrier modulation (MCM) is to facilitate the transmission of data by dividing the stream into a number of individual bit streams, each of which has a considerably lower bit rate, and then employing those individual bit streams as the modulating source for more than one carrier. In wireless communication systems and telecommunications, multicarrier modulation is a technology that allows data to be transmitted simultaneously via many subcarriers. It works especially well to counteract frequency-selective fading, which can seriously deteriorate wireless channel signal quality. The data stream to be sent is split up into several concurrent sub-streams in multicarrier modulation, and each of these sub-streams is modulated onto a different subcarrier. These subcarriers span the available bandwidth and are usually closely spaced. Multiple carrier modulation techniques, such as filter bank multicarrier (FBMC) and orthogonal frequency division multiplexing (OFDM), (Pranathi & Naveena, 2023).

The primary means of addressing certain 5G characteristics that 4G is unable to adequately handle is thought to be the multicarrier modulation technology. Higher data rates (up to 10 Gbps), less latency, increased capacity, and extended battery life are some of these features. In 4G, OFDM is a multicarrier modulation method. Its advantages lower implementation complexity, greater adaptability in accommodating adaptive subcarrier modulation, and easier equalization and channel estimation processing combined with a number of drawbacks render it less effective in meeting 5G standards. In addition to having cyclic prefix (CP), which limits spectral efficiency, OFDM also has a long trip time, which reduces its efficiency in machine-to-machine (M2M) applications. It also has high out-of-band emission (OOB), which is caused by the large power of the side lobe. All of these factors make OFDM difficult to synchronize and interfere with inter-symbolic communication. Therefore, it is imperative that a new multicarrier modulation be used in 5G to replace OFDM. Given its many positive qualities, FBMC is a potential substitute multicarrier modulation for OFDM in 5G networking. For instance, it excludes CP in favour of adding extra filtering at TX and RX in addition to IFFT/FFT. This is achieved by filtering each FFT output using a frequency version of an LPF known as a prototype filter, which increases bandwidth efficiency. Furthermore, FBMC is more resilient to synchronization and frequency misalignment and more adaptable in utilizing white spaces in cognitive radio networks. (Abouldahab et al., 2018).

The prevalent transmission method in use in today's wireless systems, orthogonal frequency division multiplexing (OFDM), is meant to continue to be useful in the upcoming fifth generation of wireless systems. Nonetheless, in recent years, there has been a rise in interest in alternative systems such Filter Bank Multicarrier Modulation (FBMC) with Offset Quadrature Amplitude Modulation (OQAM). When compared to OFDM, FBMC offers far superior spectrum qualities; nevertheless, it also has some extra drawbacks, such as less compatibility with multiple-input multiple-output (MIMO) systems. Furthermore, a high Peak-to-Average Power Ratio (PAPR) is a disadvantage shared by all multi-carrier designs. However, one of the main benefits of multi-carrier systems is that the equalization process may be made a lot simpler because one-tap channels can typically represent the transmission over a time-variant multi-path channel (Nissel et al., 2018).

1.2 Motivation

The motivation of the study encompasses the performance evaluation of a channel estimation method for doubly-selective fading channel in the context of Filter Bank Multi-Carrier (FBMC) high order QAM modulation, with a specific focus on its applicability to 5G wireless networks. The study aims to address the challenges posed by time and frequency variations in the channel by leveraging the time and frequency correlation of scattered pilots. The study includes the performance evaluation of different channel estimation techniques such as Minimum mean Square Error, Least square, Constructed data pilot and Spectral Temporal Average and prototype filters for doubly-selective fading channel in the context of Filter Bank Multi-Carrier (FBMC) high order QAM modulation. This is crucial in meeting the increasing demands for higher data rates, improved spectral efficiency, and enhanced reliability in the next generation of wireless networks. Furthermore, the research demonstrates the versatility of the channel estimation method across different multicarrier modulation techniques, including Orthogonal Frequency Division Multiplexing (OFDM), UFMC, WOLA and FBMC. This versatility expands the applicability of the method beyond FBMC systems, making it a valuable tool for channel estimation in various communication systems. By analysis different prototype filter and channel estimation technique for doubly-selective fading channels in Filter Bank Multi-Carrier (FBMC) modulation, the research contributes to the development of more efficient, low out of band emission and high-performing communication systems for 5G networks.

As a result, this thesis focuses on evaluating the performance of different alternatives of prototype filter, and sub-carrier spacing which is ultimately reduce the out of band emission/OOB/ and asses the performance of different multicarrier modulation techniques.

1.3 Statement of Problem

The advent of 5G wireless communication and the anticipated transition to future communication technologies have brought about the need for advanced channel estimation techniques. In particular, the use of Filter Bank Multi-Carrier (FBMC) modulation combined with higher order Quadrature Amplitude Modulation (QAM) presents a promising approach for achieving high data rates and spectral efficiency. The performance of FBMC systems in frequency-selective fading channels, known as doubly selective channels, greatly depends on the prototype filter. The complexity of doubly selective channels arises from their time-varying and frequency-selective nature, which poses significant challenges for accurate channel estimation. By conducting a comprehensive analysis, this research aims to provide valuable insights into the performance trade-offs and limitations of different channel estimation techniques in the context of future wireless communication systems, thus guiding the design and implementation of efficient and robust communication solutions.

By conducting a comprehensive analysis, the study aims to identify the most suitable approach that effectively mitigates ISI and ICI, improves data rates, and enhances reliability in FBMC systems with higher order QAM. The findings was provide valuable insights into the performance trade-offs and limitations of different channel estimation techniques, guiding the design and implementation of efficient and robust wireless communication solutions for present and future networks.

1.4 Objectives

The objective of this thesis can be seen as General objective and Specific objective.

1.4.1 General Objective

The General objective of this research is to evaluate the Performance Evaluation of Doubly Selective Fading in FBMC with Higher Order QAM for 5G Wireless Communications and Beyond.

1.4.2 Specific Objectives

- To analyse the statistical properties of time and frequency selective fading in Filter Bank Multi-Carrier (FBMC) technique.
- To evaluate the performance of different prototype filters under doubly selective fading channel.
- To evaluate performance metrics of FBMC such as Bit Error Rate (BER) and Signal-to-Noise Ratio (SNR), with advanced modulation techniques such as UFMC, F-OFDM and WOLA technique under doubly selective fading for 5G and beyond wireless communication.

1.5 Significance of the Study

The study focuses on advancing 5G wireless networks by addressing the challenges specific to this context. By proposing a method for estimating doubly-selective channels in Filter Bank Multi-Carrier (FBMC) modulation, the research contributes to the development of more efficient and high-performing communication systems for 5G networks. This is crucial in meeting the increasing demands for higher data rates, improved spectral efficiency, and enhanced reliability in the next generation of wireless networks. Furthermore, the research demonstrates the versatility of the proposed channel estimation method across different linear modulation techniques, including Orthogonal Frequency Division Multiplexing (OFDM) and FBMC. The proposed method addresses the challenges posed by doubly-selective fading, improves estimation accuracy, and has the potential to enhance the overall performance of data communication systems. Its versatility, interference cancellation scheme, and rigorous evaluation make it a valuable tool for improving channel estimation in various communication technologies, thereby driving the progress of wireless communication systems and networks.

1.6 Scope of the Study

The scope of the study encompasses the development and evaluation of a novel channel estimation method for doubly-selective fading in the context of Filter Bank Multi-Carrier (FBMC) modulation, with a specific focus on its applicability to 5G wireless networks. The study aims to address the challenges posed by time and frequency variations in the channel by leveraging the time and frequency correlation of scattered pilots. The proposed method will be evaluated through simulations over doubly-selective channels, comparing the estimated channel knowledge with the ideal scenario of perfect channel knowledge. Additionally, the study was assess the versatility of the method across different linear modulation techniques, such as Orthogonal Frequency Division Multiplexing (OFDM) and FBMC. The scope of the study extends to providing insights into the improved accuracy and reduced interference achieved through the incorporation of an iterative interference cancellation scheme. Overall, the study has a comprehensive scope that encompasses the development, evaluation, and applicability of the proposed channel estimation method in the context of FBMC modulation and 5G wireless network.

1.7 Thesis Contributions

The main contributions in this work are related to the comparison and performance evaluation of FBMC channel estimation for high order QAM in doubly selective fading channel with other multicarrier modulation techniques, prototype filter selection which provides limited OOB. The main work in this contribution is summarized as follows:

- The BER performance of FBMC high order QAM in doubly selective fading channel is compared. Slow fading channel model/pedestrian/ and fast fading channel/vehicular/ channel model is considered.
- Different multicarrier modulation technique such as filtered-OFDM, WOLA, UFMC, OFDM performance of BER compared against FBMC with high order QAM modulation under doubly selective fading channel is analysed.

1.8 Limitation of the Study

This thesis limited to simulation of the system which is done using application software called MATLAB.

1.9 Thesis Organization

The outline of this thesis is summarized as follows:

Chapter one: This chapter mainly focuses on the background of the study, statement of the problem, objectives, contribution of the study, scope of the study, and limitations of the study.

Chapter Two: presents different researchers work regarding on FBMC and multicarrier modulation techniques performance and channel estimation techniques.

Chapter Three: describes the research methods used in this thesis including the derivation of performance metrics for FBMC/QAM, various channel estimation techniques, polyphase structure of synthesis and analysis filter banks different multicarrier modulation techniques such as WOLA, filtered-OFDM , OFDM and UFMC.

Chapter Four: is devoted to discuss the proposed results and discussions.

Chapter Five: presents the conclusions and recommendations.

CHAPTER TWO

2. LITERATURE REVIEW

2.1 Overview

In this chapter, some related literature is reviewed on the Performance Evaluation of Doubly Selective Channel Estimation in FBMC technologies which are directly related to the objective of this study.

2.2 Related Work

In (Dumari et al., 2023) the performance of multicarrier modulation techniques like F-OFDM, WOLA-OFDM, UFMC, FBMC with OQAM using PHYDYAS filter, FBMC with QAM using PHYDYAS filter, and FBMC with QAM using Hermite filter is compared to that of existing OFDM. The analysis is carried out based on power spectral density and bit error rate. The bit error rate analysis is carried for Vehicular A, Vehicular B, and Pedestrian B channel models at 64 QAM, 256 QAM, and 1024 QAM. The performances of different multicarrier modulation techniques are assessed in terms of their potential to fill the major requirements of new communication networks.

In(He et al., 2019) the authors first present the coding technique for canceling intrinsic imaginary interference. Next, a new technique called sparse adaptive subspace pursuit (SASP) is put out to raise the LS channel estimation's precision. Lastly, they create two unique methods for estimating channel frequency response (CFR) in the FBMC-OQAM system: coding-SASP and auxiliary pilot-SASP. Comparing the AP-SASP and coding-SASP algorithms to traditional orthogonal matching pursuit (OMP) and regularized OMP (ROMP) approaches, the results demonstrate that the former can provide a lower level of complexity and require fewer measurements. Furthermore, for the FBMC system in the doubly selective channels, the suggested AP-SASP and coding-SASP algorithms perform better in terms of bit error ratio (BER) than the traditional OMP and ROMP approaches. In this study only consider Vehicular-B and pedestrian-B channel.

In (Chen-Hu et al., 2017) Data rates for wireless broadband communication networks are constantly increasing. They should offer cutting-edge techniques that can increase spectral efficiency and more effectively repurpose the radio spectrum resources in order to accomplish this goal. The authors suggest combining FBMC-OQAM and ST in order to decrease out-of-band emissions and achieve even greater improvements in spectral efficiency. This additional improvement is the result of using the well-thought-out prototype filter that was previously discussed in relation to FBMC-OQAM. They also suggest a brand-new method for channel estimation that incorporates self-interference cancellation. Ultimately, the system's performance is assessed by comparing the MSE of the SER and channel estimate to the Auxiliary Pilot (AP) approach. However, it is ineffective in terms of the system's overall symbol error rate (SER) or mean square error (MSE) of the channel estimate.

Orthogonal frequency division multiplexing, or OFDM, has become popular in wireless communication because of its high data rate transmission capabilities and resilience to multipath fading. On the other hand, Doppler frequency shifts in mobile systems and multi-path fading significantly reduced the performance of OFDM systems, leading to inter-carrier interference (ICI). Pilot tones are introduced into each OFDM signal at the receiver in order to estimate the channel parameters using a pre-designed estimator. In this study, randomly generated pilot data is placed at equal distances from each OFDM signal.

In (Abboud & Sabbar, 2020) the Discrete Fourier Transform (DFT) is used to propose a performance test of the Least Square (LS) and Linear Minimum Mean Square (LMMSE) estimation methods based on both LS and LMMSE. Various ITU channel models are taken into consideration to compare their performance for data transmission in high mobile systems with different Doppler frequencies exceeding 200 Hz and a minimum number of pilots. However, this work does not take into account the trade-off between BER improvement and estimation complexity when using high Doppler frequencies and fewer.

In (Hosseiny et al., 2020), the B system uplink is taken into consideration by the researcher. For FBMC, they provide a collaborative multiuser channel estimation technique as well as a pilot structure. By spacing out the users' pilots in terms of frequency and time, their suggested pilot structure lowers the overhead associated with training. As a result, they increase spectral efficiency and can handle more training signals in the same bandwidth. In addition, this pilot structure naturally results in a lower peak-to-average power ratio (PAPR) as compared to methods that train using all of the subcarriers. Their suggested approach, which relies on its enhanced spectral efficiency, can alleviate the pilot contamination issue in FBMC-based massive MIMO systems while catering to a high number of users. Simulation results in terms of sum-rate performance for single- and multi-cell scenarios support this. This study does not analyse the performance of bit error rate (BER) and complexity of system.

In (Wang et al., 2023), the authors introduce an ICI/ISI mitigation strategy for the offset quadrature amplitude-modulated filter bank multi-carrier (OQAM-FBMC) system. Broadband transmission systems have difficulties with equalization and channel estimation across a doubly selective channel. Inter-carrier interference (ICI) is caused by high mobility, whereas inter-symbol interference (ISI) is caused by multipath transmission. It has a high efficiency and a low inherent imaginary interference (IMI) sensitivity. In particular, two algorithms are proposed based on the 2-D channel modelling scheme: a sparse adaptive orthogonal subspace pursuit (SAOSP) technique and a pilot indices optimization approach. To lessen the impact of ICI, guard pilots are added first. Next, in order to obtain a high-accuracy estimation of sparse channel coefficients, the index optimization and SAOSP techniques are utilized. Furthermore, a threshold judgment suboptimal minimal mean square error (MMSE) equalization technique based on interference power fluctuation is described. The technique estimates the ISI dimension and reduces the equalization data using normalized interference power thresholds, minimizing the impact of ISI and delivering effective equalization.

In (Sim & Lee, 2019) the authors assess the effectiveness of two prototype filters in a filter bank multicarrier-quadrature amplitude modulation (FBMC-QAM) system. For additive white Gaussian noise channels and multipath fading channels, they examine the effective channel and calculate the signal-to-interference ratio. Investigated are the properties of the effective channel as per different prototype filter sets and channel models, based on the analysis. Then create two different kinds of per-tone channel equalizers using the effective channels, and then use Monte Carlo simulations to assess the bit error rate performances. According to results, by using the signal-level per-tone channel equalization, the FBMC-QAM system with two prototype filters may nearly reach the same bit error rate performance as orthogonal frequency division multiplexing with a cyclic prefix. Finally, analysis is conducted on the computational complexity of per-tone channel equalizers. But this study does not analyse other parameters like, PAPR or spectral efficiency.

Peak to Average Power Ratio and Bit Error Rate Analysis of MultiCarrier Modulation Techniques is studied in (Marian Joseph Jeffery et al., 2020). This paper compared three different multi-carrier modulation techniques: OFDM, SC-OFDM, and FBMC. FIR filters are implemented in FBMC using Poly-Phase Networking (PPN) filter banks. As a result, the wideband signals are broken down into narrowband signals, which lowers the system's PAPR overall. Performance measures like as Signal to Noise Ratio (SNR), BER, and PAPR are employed in the analysis of OFDM, SC-FDMA, and FBMC. Performance metrics are compared for several channels, such as Rayleigh, Rician, and Double Selective, and their impact on modulation schemes is discussed; nevertheless, the examination of spectral efficiency, complexity, and signal to interference ratio is left out.

In (Kassaw, 2019) the comparative performance analysis of modulation formats for 5G Wireless system is provided. In this research the modulation schemes of 5G wireless system like FBMC, UFMC are compared to that of CP-OFDM. The performance metric used to compare these modulation formats were BER, spectral efficiency, power spectral density and computational complexity. They provided the basic principle of the waveform and also revealed the characteristics of each wave forms. This research shows some drawback of CP-OFDM and the potential candidate modulation format that overcome the limitation of CP-OFDM. The research is limited to performance metrics like BER, spectral efficiency, PSD and computational complexity and SIR, and the like aspect not addressed and also other modulation formats for 5G.

Comprehensive analysis of UFMC with OFDM and FBMC is provided in in terms of peak average power ratio by applying different sub-carriers and modulation techniques. They try to address the advantage and drawback of OFDM and proposed FBMC and UFMC are the candidate waveforms that overcome the shortcomings of OFDM. The benefits of UFMC and FBMC are partially presented in it. They proposed UFMC as best choose. In this paper analysis is limited to PAPR but PSD, complexity, BER aspects not addressed.

In (Kishore et al., 2017) a comprehensive analysis of UFMC with OFDM and FBMC is provided in terms of peak average power ratio by applying different sub-carriers and modulation techniques. They try to address the advantage and drawback of OFDM and proposed FBMC and UFMC are the candidate waveforms that overcome the shortcomings of OFDM. The benefits of UFMC and FBMC are partially presented in it. They proposed UFMC as best choose. In this paper analysis is limited to PAPR but PSD, complexity, BER aspects not addressed.

In (Ramadhan, 2019) Here is the implementation of the FBMC (New Multicarrier Modulation Technique) and 5G Filtered-OFDM Waveform Candidate. The fundamental multi-carrier modulation method for cellular and wireless communications is known as OFDM. For point-to-point communication, OFDM is the ideal option since it produces very high bandwidth with the least amount of complexity. It does, however, face a number of difficulties, including significant out-of-band emissions and low spectral efficiency. These days, a number of modulation approaches are being developed to address these issues; one such technique is Filter Bank Multi Carrier (FBMC).

In (Nissel, 2016) By computing the Bit Error Probability, the performance of OFDM and FBMC-OQAM in Doubly-Selective Channels is taken into consideration. To compute the BEP in doubly-selective channels for arbitrary linear modulation schemes based on one-tap equalizers, such FBMC or OFDM, a compact framework is presented. Additionally, although the bit mapping can be random, there is Rayleigh fading, perfect channel knowledge at the receiver, and the data symbols are selected from a constellation of m-Quadrature Amplitude Modulation (QAM) signals.

Table 2.1 Contribution and gap of different related works.

Title	Contribution	Gap
OFDM and FBMC-OQAM in Doubly-Selective Channels: Calculating the Bit Error Probability (Nissel & Rupp, 2017)	The analysis is focused on BEP and SNR comparison of FBMC-OQAM in doubly selective channel	The complexity aspect not addressed. Effect of high order QAM not considered.
Implementation of a 5G F-OFDM and FBMC Modulation Techniques (Ramadhan, 2019)	Wave-forms like F-OFDM and FBMC studied	Other wave forms that have comparable performance like WOLA-OFDM, UFMC not addressed
Characteristic Analysis of OFDM, FBMC and UFMC Modulation Schemes for Next Generation Wireless Communication(Kundrapu et al., 2019)	The analysis is focused on spectral efficiency, bit error rate, peak average power ratio by utilizing various sub-carriers and modulation techniques	Complexity of aspect not addressed.
Peak to Average Power Ratio and Bit Error Rate Analysis of MultiCarrier Modulation Techniques (Marian Joseph Jeffery et al., 2020)	Performance Metrics are compared across various channels like Rayleigh, Rician and Double Selective and their influence on the modulation techniques	Complexity of aspect not addressed.

Spectrally Efficient Pilot Structure and Channel Estimation for Multiuser FBMC Systems (Hosseiny et al., 2020)	increase spectral efficiency and decrease peak-to-average power ratio. .	This study does not consider the performance of bit error rate (BER) and complexity of system.
Performance evaluation of high mobility OFDM channel estimation techniques (Abboud & Sabbar, 2020)	DFT is used to propose a performance test of the LS and LMMSE estimation methods based on both LS and LMMSE	this work does not take into account the trade-off between BER improvement and estimation complexity when using high Doppler frequencies and fewer pilots .
Doubly selective channel estimation and equalization based on ICI/ISI mitigation for OQAM-FBMC systems (Wang et al., 2023)	By using sparse adaptive orthogonal subspace pursuit (SAOSP) technique to mitigate ICI and ISI.	Complexity of aspect not addressed.

CHAPTER THREE

3. Material and Methodology

3.1 Material

Software materials used in this thesis are MATLAB R2021a, EDRAW MAX and MS Word EDRAW MAX is used to draw block diagrams, figures. MATLAB R2021a, which is a computing software that consists of Editor, which is used to write a code and do mathematical computation.

3.2 Methodology

There should be a method to be followed to attain any goal. Thus, the following methods and techniques are going to be followed to attain the above listed general and specific objectives of the study.

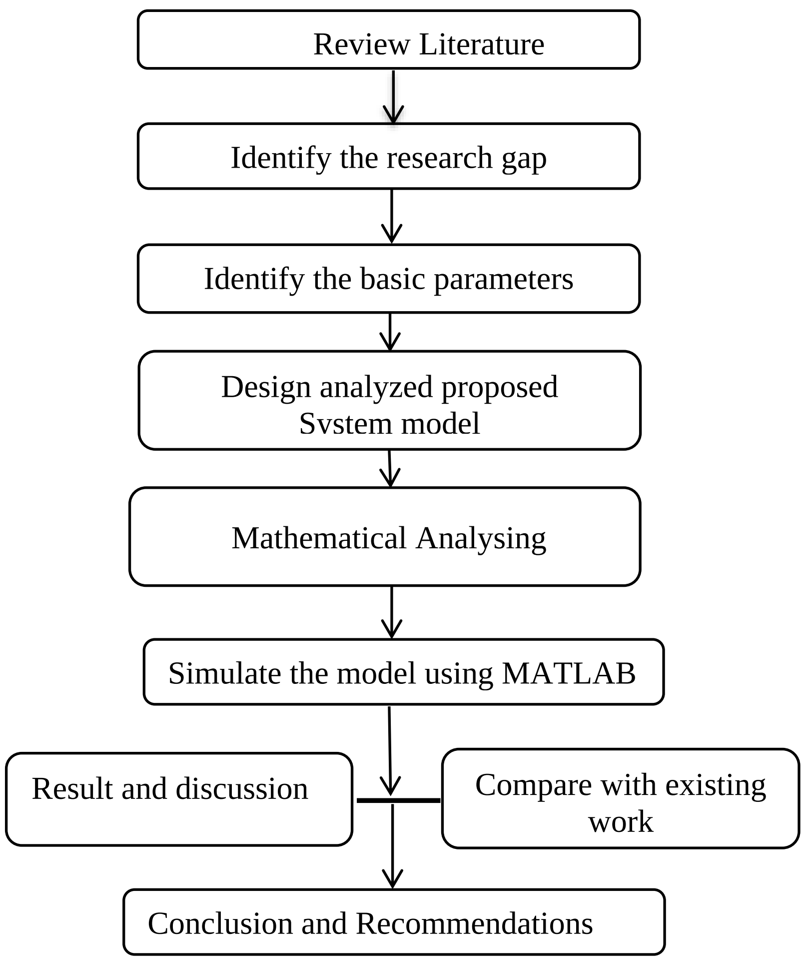

Figure 3.1 Thesis work flow

3.3 Description of the system

3.3.1 Multicarrier Modulation

The practise of altering one or more characteristics of the carrier signal a periodic waveform is known as modulation. The multicarrier modulation was considered as an effective way to attain high data rate transmission. This is because the total channel bandwidth was divided into sub-channels with subcarriers will be modulated with a lower data rate. To achieve high speed data transmission, these lower data streams will be transmitted simultaneously through the subcarriers after modulation(Sim & Lee, 2019). Analogue modulation applies a continuous modulation in response to an analogue information signal. An analogue carrier signal is modulated by a discrete signal in digital modulation. There are two categories for this modulation technique: single and multicarrier. Unlike multicarrier modulation, which splits the entire frequency channel into many sub-carriers and transmits the high-rate data stream in parallel on sub-carriers, single carrier modulation systems employ a single signal frequency to send data symbols. A multicarrier method is one in which data symbols are sent concurrently across more than one frequency subcarrier. There are different type of multicarrier modulation such as, Filter bank multicarrier and orthogonal frequency division multiplexing.

3.3.2 Orthogonal Frequency Division Multiplexing

Multicarrier OFDM systems accomplish orthogonality between the various subcarriers and overlap the frequency spectrum of the subcarriers with the fewest frequencies. Chang is the creator of OFDM. If there is a substantial overlap between the signal bands, there won't be any interference between orthogonal transmissions (He et al., 2019). Multiple subcarriers that can transport different kinds of data over a range of frequencies can be formed by using OFDM. These subcarriers would all need to be perpendicular. When a function's integral over a given time interval is zero, it is said to be orthogonal mathematically. Broadband signals often have a limited range due to their frequency-specific transmission channels. A frequency selective channel can be countered using an OFDM approach (He et al., 2019). To create N frequency flat channels in OFDM, the entire bandwidth of a frequency selective channel is split into N sub bands with equal spacing. Because the modulation's carriers are orthogonal, there is no interference. The transmitter employs IFFT to do this. Using FFT, the receiver retrieves the data. Because the OFDM waveform has a wide sideband, choosing the next channel still requires using the guard band. Guard bands reduce the effectiveness of OFDM. In this way, FBMC a novel technique for raising spectral efficiency was created. An IFFT is utilized in FBMC to improve the waveform's spectral efficiency. One of the main issues with OFDM is its greater PAPR (Sim & Lee, 2019).

3.3.3 Filter Bank Multi-Carrier (FBMC)

Compared to conventional Orthogonal Frequency Division Multiplexing (OFDM), Filter Bank Multi-Carrier (FBMC) communication has garnered global attention recently due to its enhanced spectrum efficiency, flexibility, and improved spectral confinement (Abbas et al., 2023). With more advanced filtering methods, FBMC achieves higher spectrum efficiency than OFDM. Prototype filters with improved spectral containment characteristics allow FBMC to reduce interference between neighboring sub-bands and allocate a more focused portion of the available frequency spectrum. When well-designed prototype filters are used, FBMC naturally reduces out-of-band emissions. These filters reduce spectral leakage between sub-bands, which helps to enhance spectral confinement and reduce interference with adjacent channels. It is possible to develop FBMC to accommodate a large variety of system requirements and specifications. Different constellations and modulation orders are offered, along with a multitude of modulation forms.

Mathematically, the transmitted signal, *s(t)*, of a multicarrier system in the time domain can be expressed as

$$S(t) = \sum_{k=1}^{K} \sum_{l=1}^{L} g_{l,k}(t) x_{l,k}(t) \tag{3.1}$$

where $x_{l,k}$ denotes the transmitted symbol at subcarrier-position l and time-position k, and is chosen from a symbol alphabet X, often a QAM constellation. The transmitted basis pulse, $g_{l,k}(t)$ in Eq. (3.1), is defined as

$$g_{l,k}(t) = P_{TX}(t - kT) e^{j2\pi F(t-kT)} e^{j\theta_{l,k}}, \tag{3.2}$$

where $P_{TX}(t)$ represents prototype filter, T denote the time spacing and F indicates the frequency spacing (subcarrier spacing). In fact, the system is essentially, a time and frequency shifted version. The choice of the phase shift, $\theta_{l,k}$, becomes relevant later in the context of FBMC-QAM. After transmission over a channel, the received symbols are decoded by projecting the received signal, *r(t)*, onto the receive basis pulses, $q_{l,k}(t)$, that is

$$y_{l,k}(t) =< r(t), q_{l,k}(t) >= \int_{-\infty}^{\infty} r(t)\, q^*{}_{l,k}(t) dt \tag{3.3}$$

where $q_{l,k}(t)$ is similarly defined as $g_{l,k}(t)$, except that a different prototype filter might be used:

$$q_{l,k}(t) = P_{TX}(t - kT)e^{j2\pi IF(t-kT)}e^{j\theta_{l,k}} \tag{3.4}$$

In an Additive White Gaussian Noise (AWGN) channel, a matched filter maximizes the SNR, that is, $q_{l,k}(t)$ = $g_{l,k}(t)$ and thus $P_{RX}(t)$= $P_{TX}(t)$. In a doubly-selective channel, on the other hand, the *TX* prototype filter and the *RX* prototype filter slightly differently, $P_{RX}(t) \neq P_{TX}(t)$, as expressed in pulse-shaped multicarrier transmissions (Matz et al., 2007) or in the practically more relevant case of CP-OFDM. As indicated in Eq. (3.1) to (3.4), multicarrier systems are mainly characterized by the prototype filters, $P_{TX}(t)$ and $P_{RX}(t)$, as well as time spacing T and frequency spacing F, so that the ambiguity function, defined as [(Hosseiny et al., 2020), (Sahin et al., 2014)].

$$A(t, v) = \int_{-\infty}^{\infty} P_{TX}(t - \frac{t}{2})P_{Rx}^{*}(t - \frac{t}{2})e^{j2\pi vt}\, dt \tag{3.5}$$

captures the main properties of a multicarrier system in a compact way. The projection of the transmitted basis pulse onto the received basis pulse can then be expressed by the ambiguity function as

$$g_{l1,k1}(t), q_{l2,k2}(t) = e^{-j\pi TF(l1+l2)(k1-k2)}\, e^{j(\theta_{\,l1,k1}-\theta_{\,l2,k2})}A(T(k_1 - k_2), F(l_1 - l_2)) \tag{3.6}$$

There exist fundamental limitations for multicarrier systems, as formulated by the Balian Low theorem (Zimmermann, 1998) which states that it is mathematically impossible that the following four desired properties are fulfilled at the same time:

1. Maximum symbol density

$$TF = 1 \tag{3.7}$$

2. Time-localization

$$\sigma_t = \sqrt{\int_{-\infty}^{\infty} (t - \dot{t})^{2}\, |P(t)|^2 dt} < \infty \tag{3.8}$$

3. Frequency-localization

$$\sigma_f = \sqrt{\int_{-\infty}^{\infty} (f - \dot{f})^{2}\, |P(f)|^2 df} < \infty \tag{3.9}$$

4. (Bi)-orthogonality

$$< g_{l1,k1}(t), q_{l2,k2}(t) = \sigma_{(l1-l2),(k1-k2)} \tag{3.10}$$

$$A(T(k1-k2), F(l1-l2)) = \sigma_{(l1-l2),(k1-k2)} \tag{3.11}$$

with δ denoting the Kronecker delta function. The pulse

$$P(f) = \int_{-\infty}^{\infty} p(t) e^{-j2\pi f t} dt \tag{3.12}$$

In Eq. (3.12) represents the Fourier transform of $P(t)$ while t = $\int_{-\infty}^{\infty} t\, |p(t)|^{2}\, dt$ corresponds to the mean time and f = $\int_{-\infty}^{\infty} t\, |p(f)|^{2}\, df$ the mean frequency of the pulse. The localization measures in Eqs. (3.8) and (3.9) can be interpreted as standard deviation with $|p(t)|^{2}$ and $|p(f)|^{2}$ representing the probability density function *(pdf)*. This relates the Balian-Low condition to the Heisenberg uncertainty relationship. There does not exist a unique definition for FBMC-QAM. Some authors (Nam et al., 2016) sacrifice frequency localization, making the modulation scheme even worse than OFDM in terms of OOB emissions. Others (Yun et al., 2015),(Kim et al., 2016) sacrifice orthogonality in order to have a time-frequency spacing of *TF* ≈ 1 and time-frequency localization. Increasing *TF*, FBMC-QAM a time-frequency spacing of *TF* = 2, sacrifice spectral efficiency to fulfil all other desired properties. Such large time-frequency spacing increases the overall robustness in a doubly-selective fading channel.

Filter banks are added to the OFDM system to address some of its drawbacks, and the filter bank based multicarrier (FBMC) eliminates the CP to increase system flexibility. A filter bank can have a variety of designs to meet the needs of a communication system, including reducing sideband power loss and enhancing spectral efficiency. Because subcarrier filters are narrow in frequency and the symbols overlap over time, they need long filter lengths (often at least 4T) to maintain an acceptable ISI and ICI. Data can be sent randomly in QAM, so that, in the constellation diagram for 4-QAM, which has many amplitude changes, 00 can be followed by 11 (a diagonal transition).

Nevertheless, transmission bursts at both ends, transition times (tails) with a duration equal to the prototype filter length, and the T=2 time offset between QAM symbols induce overhead for FBMC/OQAM (Nissel et al., 2018). The discrete time FBMC-QAM system's transmitted signal is expressed as follows.

$$s(n) = \sum_{-\infty}^{\infty} \sum_{P} a_{p,k} g^{e}[n-kM]\ e^{j2\pi/Mm(n-D)} + \sum_{P} a_{p,k} g^{o}[n-kM] e^{\frac{j2\pi}{Mm(n-D)}} \tag{3.13}$$

Where $g^e[n]$ represent even filter, $g^o[n]$ represent odd filter and $a_{p,k}$ represent a complex data symbol in terms of QAM constellation. indicated the time index, m represents the subcarrier index, k indicates the symbol index, $d_{m,k}$ represents the real valued symbol, M represents the number of subcarriers, and $f(n)$ shows the synthesis impulse response, which maps $d_{m,k}$ in to the signal space. $a_{p,k} = j^{k+m}$ $k + m$ is the additional phase term. The filter delay, which is represented by D, appears to generate a causal discrete time prototype filter f_n , and it is fxed $D = (L - 1)/2$ with filter length equal to L as in (Andrews et al., 2014).

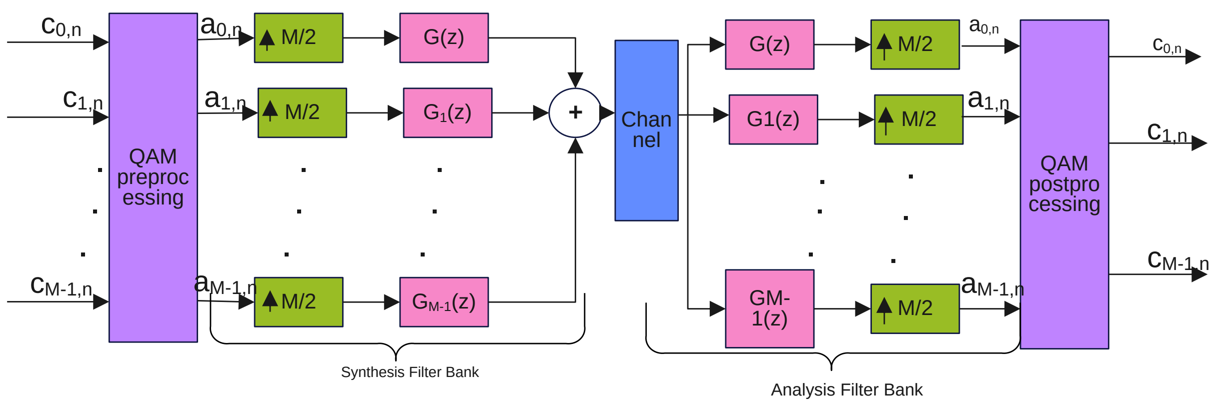

Figure 3.2 FBMC Synthesis and Analysis filter bank model

The prototype filter that determines the system's performance, including stop-band attenuation, inter-carrier interference (ICI), and inter-symbol interference (ISI), is usually used to build the filter banks that contain synthesis and analysis filters. It is necessary to carefully build the prototype filter in order to remove ISI and ICI and maintain modest side lobes. The prototype filters are developed utilizing polyphase implementation, which combines the implementation of all analysis or synthesis filters in the filter bank to minimize complexity through the use of multi-rate signal processing techniques. The transmitted signal is the sum of a M filters bank the outputs in the FBMC. with filter length $L = M \times O$, where M is the FFT size and O is the prototype filter overlapping factor.

When comparing FBMC to OFDM, the more sophisticated prototype filter design allows for more sub-carrier localization and detachable CP, which boosts spectral efficiency. Furthermore, there is a significant increase in spectral efficiency because of the FBMC's smaller guard band. QAM pre-processing, synthesis filter bank, analysis filter bank, and QAM post-processing are the primary processing steps of the FBMC system in direct form representation.

3.3.4 Synthesis and analysis filter banks

All sub-signals are added together to form the SFB output signal at the transmitter end. All sub-sub-carrier filters are created from a low pass prototype filter $g(m)$ with single real-valued linear-phase by using exponential modulation in the case complex modulated filter banks class is chosen. At the transmitter side, the symbols $a_{k,n}$ are up-sampled by M/2 and up-sampled signals are then filtered with their analogous filter $G_k[z]$ to give M sub-channels in the SFB block. Because of the modulation function, the resulting sub-channel filters have complex values, and as a result, the useful frequency band is [−π, π]. Generally, even-stacked filter banks and odd-stacked filter banks are the two different channel kinds that can be taken into consideration when assembling preparations. (Alhava & Renfors, n.d.). The k^{th} sub-channel filters centre frequencies are $w_{k=}\ \frac{2k\pi}{M}$ and $w_{k=}\ \frac{(2k+1)\pi}{M}$ for even stacked and odd-stacked filter banks, respectively. The k^{th} synthesis filter is given by,Eq. (3.14)

$$g_k[m] = g[m]e^{\left(j\frac{2\pi k}{M}(m-\frac{L_p-1}{2}\right)} \tag{3.14}$$

where Lp is the filter length and m = 0, 1,..., Lp−1. It is believed that the prototype filter is designed so that additional scaling factor is not required to make representations simpler. The analogous synthesis filter complex-conjugated version, as provided in Eqs, (3.15–3.17) is the k^{th} analysis filter, which is simply a time-inverted version.

$$f_k[m] = \ g_k^*[L_p - 1 - m] \tag{3.15}$$

$$= \ g_k[L_p - 1 - m]e^{(-j\frac{2\pi k}{M}(L_p-1-m-\frac{L_p-1}{2}} \tag{3.16}$$

$$= \ g[m]e^{(j\frac{2\pi k}{M}(m-\frac{L_p-1}{2}} \tag{3.17}$$

3.4 Polyphase Implementation

Because filtering operations are carried out at a high sample rate that leads to a significant number of undesired calculations, the direct form implementations are not well organized for practical applications. Fortunately, a variety of effective multirate structures, including lattice, polyphase, and lapped transform structures, are required for the filter banks (Vaidyanathan, 1993). For Nearly Perfect Reconstruction (NPR) filter banks, only polyphase architectures are suitable. Their primary advantage is their ability to provide extreme oversimplifications due to the fact that desired computations are performed and filtering operations are carried out at a reduced sampling rate.

3.4.1 Polyphase structure of synthesis filter bank

With M sub-carriers in the synthesis filter bank and a frequency gap of Δf between them, the signal bandwidth$B_w = M\Delta f$ is obtained. The sampling theorem states that the sampling interval Ts equals the inverse of the signal bandwidth (Ts = 1/Bw = T/M). Since the length of a symbol period is T, the number of corresponding signal samples for each symbol period is T/Ts = M. The discrete-time prototype filter is obtained within a sampling rate of Ts by sampling the continuous-time prototype filter g(t), leading to (3.18)

$$g[m] = g(mT_s), \qquad m = 0,1 \dots L-1 \tag{3.18}$$

where L is the length of the discrete-time prototype filter $g_T[m]$, and it is possible for the prototype filter length to exceed the symbol period. Assuming that *O* is the overlapping factor, the prototype filter length is equal to *O* times the symbol period, or *L = OM*. The Z-transform, a crucial analysis technique in communication systems, transforms the discrete-time signal into a complex frequency domain. The $g_T[m]$ *Z-transform* is determined by Eq. (3.19)

$$G[z] = \sum_{m=0}^{L-1} g(m)z^{-m} = \sum_{m=0}^{ON-1} g(m)z^{-m} \tag{3.19}$$

Letting $m = l'm + k'$ m, where $l' = 0,1, \dots. O-1$ and $k' = 0,1, \dots \dots (M-1)$ Eq. (3.19) can be further converted into

$$G[z] = \sum_{k\prime=0}^{M-1} \sum_{l'=0}^{O} g(l'M + k')z^{-(l'M+k')} \tag{3.20}$$

$$= \sum_{k\prime=0}^{M-1} z^{-k\prime} \sum_{l'=0}^{O} g(l'M + k')z^{-(l'M)} = \sum_{k\prime=0}^{M-1} G^{k'}(Z^m)Z^{-k\prime} \tag{3.21}$$

Where $G^{k'}(Z^m)$is polyphase filters, which is expressed as

$$G^{k'}(Z^m) = \sum_{l'=0}^{O} g_T(l'M + k')z^{-(l'M)} \tag{3.22}$$

The poly-phase filter number branches depends on the modulation function periodicity in the modulated filter banks. The modulation function periodicity used in Eqs. (3.14) and (3.17), i.e.

$$e_k[m] = e^{(j\frac{2\pi k}{M}(m-\frac{L_p-1}{2})} \tag{3.23}$$

$$= e^{(-j\frac{2\pi k}{M}\left(\frac{L_p-1}{2}\right))} e^{(j\frac{2\pi km}{M})} = \beta_k e^{(j\frac{2\pi km}{M})} \tag{3.24}$$

Then in the poly-phase filters form, the k^{th} synthesis filter can be defined in as follows

$$G_k[z] = \sum_{m=0}^{L-1} g(m)e_k[m]z^{-m} \qquad (3.25)$$

$$= \sum_{k\prime=0}^{M-1} \beta_k e^{(j\frac{2\pi k(k')}{M})} z^{-k\prime} \sum_{l'=0}^{O} g\,(l'M + k')\; z^{-(l'M)} \qquad (3.26)$$

$$= \sum_{k\prime=0}^{M-1} \beta_k e^{\left(j\frac{2\pi k(k')}{M}\right)} z^{-k'} G^{k'}(Z^M) \qquad (3.27)$$

3.4.2 Analysis filter bank poly-phase structure

The analysis filters are expressed using accurately the similar derivation as the synthesis filters. Therefore, the k^{th} analysis filter poly-phase decomposition can be directly expressed as follows:

$$\mathrm{F}_k[z] = \sum_{m=0}^{L-1} \beta_k e^{\left(j\frac{2\pi k(k')}{M}\right)} \mathrm{e}_k[m]\; z^{-m} \qquad (3.28)$$

$$= \sum_{k\prime=0}^{M-1} g_m \mathrm{e}_k[m]\; z^{-k'} G^{k'}(z^N) \qquad (3.29)$$

It is possible to understand the AFB as consisting of down-samplers by *M/2*, delay chain, IDFT, type-1 poly-phase filters, and β_k-multipliers. It is evident that the down-samplers by *M/2* are passed via polyphase filters, IDFT, and β_k-multipliers. The outcome is the polyphase implementation structure, which is identical to the synthesis filter bank. Similar primary processing blocks can be completed in reverse order, much as when synthesis filter banks are completed.

3.5 Computational complexity FBMC System

Compared to traditional OFDM, FBMC has more computational complexity despite its many benefits. Any multicarrier scheme's computational complexity can be measured by counting the real multiplications needed to compute an output sequence with length N complex values. The IFFT and FFT procedures of OFDM are what cause its computational complexity, which can be expressed as (A. Viholainen, M. Bellanger, n.d.p 22)

$$C_{OFDM} = 2 \times [NLog2N \;\times\; 3N + 4] \qquad (3.30)$$

By computing the real multiplications involved in SFB at the transmitter and AFB at the receiver, one can assess the computational complexity of FBMC. From [(A. Viholainen, M.

Bellanger, n.d. pp. 23),], the complexity of the conventional FBMC system can be written as follows

$$C_{FBMC} = 4 \times [2N + Nlog2N - 3N + 4 + 2ON] \quad (3.31)$$

By computing the real multiplications involved in the synthesis filter bank (SFB) at the transmitter (which is the same as that of the conventional system) and analysis filter bank (AFB) at the receiver, the computational complexity of the FBMC system can be assessed.

3.5.1 Filtered Orthogonal Frequency Division Multiplexing (f-OFDM)

A filter process is used in the Filtered Orthogonal Frequency Division Multiplexing (f-OFDM) mechanism, which shapes the spectrum. This proposed waveform's prototype filter is a rectangular pulse mask of the OFDM symbol with a cyclic prefix once more. Reducing side lobe leaks requires filtering desperately. In order to address the shortcomings of OFDM, the multicarrier modulation technology known as f-OFDM adds a filtering operation (Zhang et al., 2015) .

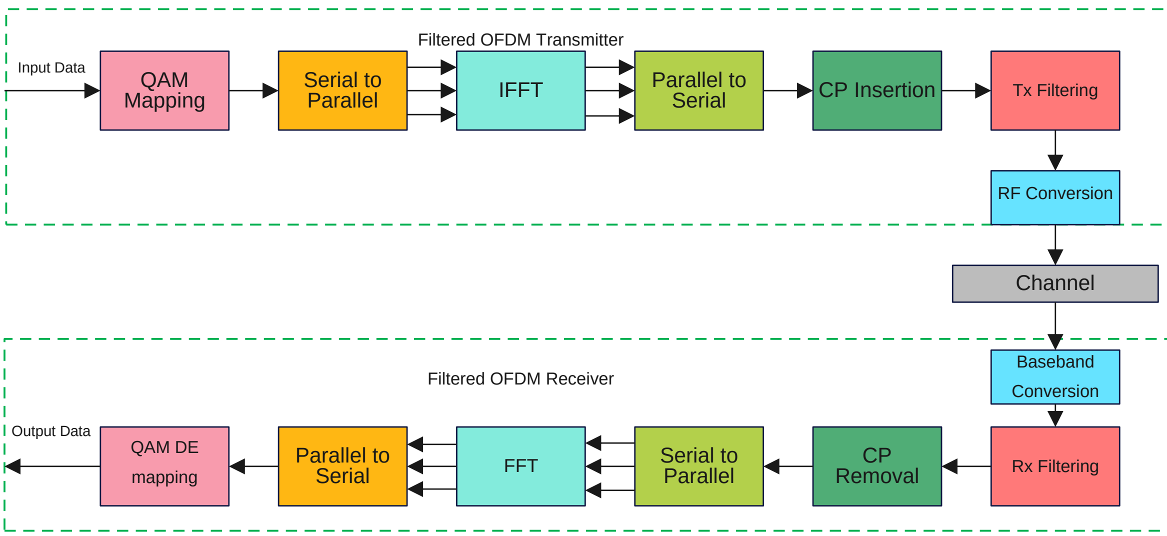

Figure 3.3 Filtered OFDM Block Diagram

The impulse response quickly disappears and the ISI is bounded in the case of the soft-truncated sinc filter, where the sinc function is soft-truncated with distinct window functions. In order to reduce inter-sub-band interference, the second type of equiripple filter structure employs the Remez algorithm, which is related to equiripple filters, to provide a finer transition band. Typically, f-OFDM's time domain expression is provided as (Bendimerad et al., 2021) .

$$X_{f-OFDM} = \frac{1}{N}\sum_{n=0}^{N-1} x_k \times f(n) \times e^{-(\frac{j2\pi nm}{N})} \quad (3.32)$$

3.5.2 Weighted Overlap and Added Orthogonal Frequency Division Multiplexing (WOLA-OFDM).

Instead of using a rectangular pulse form as is customary, a pulse with soft edges is utilized. A time domain windowing adds these soft edges to the cyclic extension. A better spectral confinement is the outcome of this. The windowing function and the OFDM symbol with cyclic prefix and cyclic suffix are multiplied point-to-point to provide a seamless transition between the last sample of one symbol and the first sample of the following symbol. (Zayani et al., 2016).

$$X_{WOLA-OFDM}(N) = \frac{1}{N}\sum_{n=0}^{N-1} x_k \times W(n) \times e^{-(\frac{j2\pi nm}{N})} \qquad (3.33)$$

where n = 0, 1, 2, . . ., $N - 1$ and $W(n)$ the discrete time domain representation of raised cosine window function can be written as in (Zayani et al., 2016). The $CP + W$ samples from the final portion of a given symbol and the first W samples from a given symbol are copied and appended to the end of the symbol to form the cyclic prefix. Therefore, from N samples to $N + CP + 2W$, the WOLA-OFDM time domain symbol is cyclically stretched. In WOLA-OFDM, a window of length $L = N + CP + 2W$ samples is applied following cyclic extension. The effectiveness of various windowing functions in boosting side lobe suppression is investigated and contrasted (Zayani et al., 2016). For WOLA-OFDM, the Meyer Root Raised Cosine is thought to offer the best windowing. WOLA-OFDM works well in reducing inter-user interference.

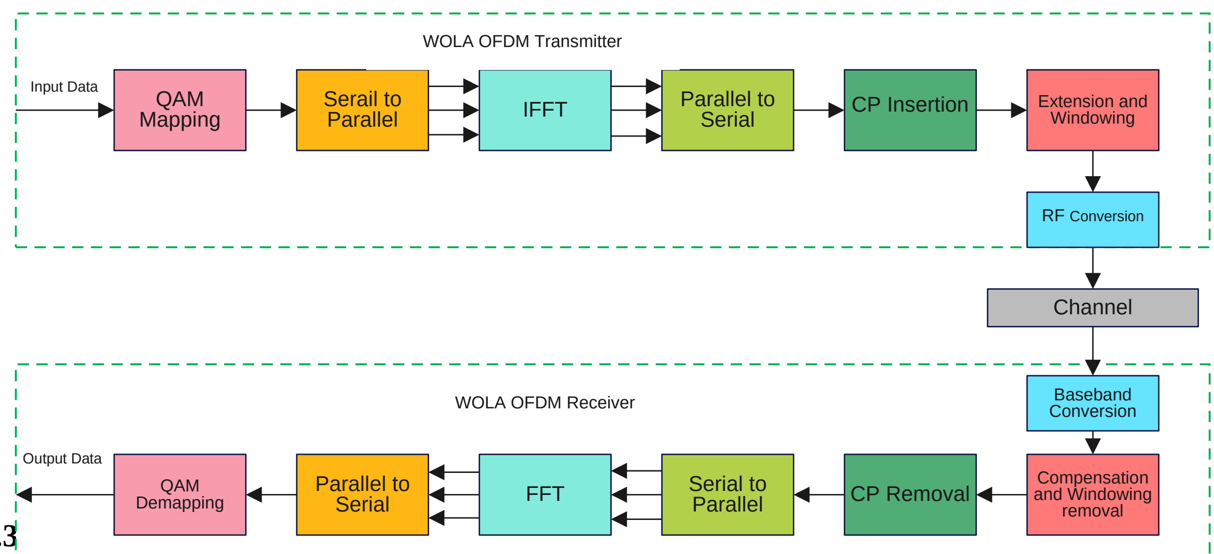

3.5.3

Figure 3.4 WOLA- OFDM Block Diagram

With sub-band filtering, the universal filtered multicarrier (UFMC) approach can be viewed as an OFDM derivative. Lower out-of-band leakage results from this post-filtering procedure than from OFDM. Every sub-band unit retains the orthogonality of its subcarriers. A technology called UFMC combines the advantages of FBMC with OFDM. Sub-bands, or groups of subcarriers, are filtered instead of filtering each carrier separately as in FBMC(Vaigandla et al., 2023), (Kamurthi & Chopra, 2018). This avoids aliasing since the filter settings and the number of carriers per sub-band are usually common. Non-contiguous sub-bands, nevertheless, are possible to enable adaptable use of the existing spectrum. As a result, UFMC can be viewed as an intermediate step between FBMC and OFDM.

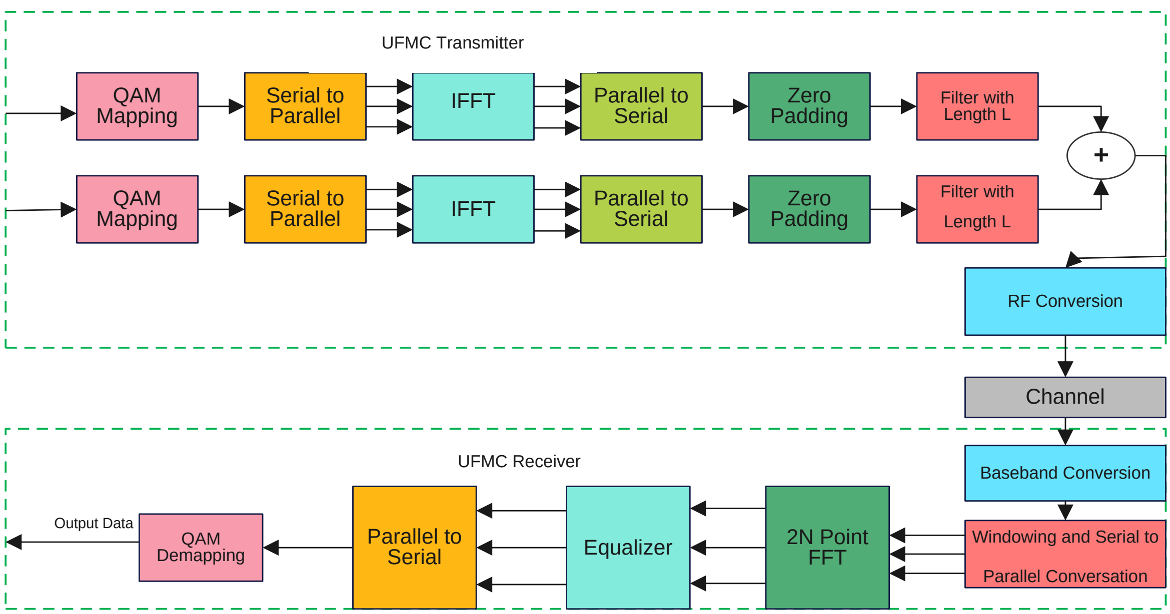

Figure 3.5 UFMC Block Diagram

Assuming that the UFMC transmit signal is split into *B* sub-bands and has *N* subcarriers. *N/B* subcarriers can be found in every sub-band. UFMC waveform generator block receives a set of constellations QAM mapped symbols as its input. The symbols S are separated into frequency blocks *S*, with *p* subcarriers making up each frequency block. The IFFT submatrix (each of dimension $N \times P$) is used to process the *B* data vectors, if *B* is the number of frequency blocks. Next, a sub-band filter of length *L* is applied to each sub-band, and the sum of the responses from each sub-band is calculated. The discrete baseband UFMC signal is expressed mathematically as in(Vaigandla et al., 2023):

$$X_{UFMC} = \sum_{K=0}^{K-1} S_k(n) * f_k(n) \tag{3.34}$$

where K is the number of sub-bands, $f_k(n)$ shows the filter coefficients in sub-band of order *k*, and $S_k(n)$ refers to the equivalent OFDM modulated signal over sub-band of order *k*.

3.5.4 Orthogonal Frequency Division Multiplexing (OFDM)

A multicarrier transmission technique called OFDM splits the frequency spectrum into several smaller channels. It is composed of an FFT block in the receiver and an IFFT block in the transmitter, respectively. The modulated N subcarriers that yield the OFDM signal have the following mathematical expression (Kassaw, 2019).

$$s(t) = \sum_{n=0}^{N-1} d_n\left(e^{j2\pi f_n t}\right) \; for\; 0 \leq t \leq T_s \tag{3.35}$$

where T_s is the time duration of OFDM symbols, which is $T_s = NT_d$, and $T_d$is the duration of the serial symbol. The complex data symbol, d_n, modulates the N^{th} subcarrier at the modulation interval. As long as there is an equal spacing between adjacent subcarrier frequencies and subcarriers are positioned at

$$f_n = \frac{n}{T_s} \quad for\;, n = 0,1,2, \dots \dots \dots N-1 \tag{3.36}$$

The received signal, r(t), obtained from the convolution of s(t) with the channel impulse response, h(t), and addition of a noise signal, n(t), is the channel's output following radio frequency conversion. (Kassaw, 2019).

$$r(t) = \int_{-\infty}^{\infty} s(t-\tau)h(\tau,t)d\tau + n(t) \tag{3.37}$$

The output of the FFT is the multicarrier demodulated sequence of N complex valued symbols (Bendimerad et al., 2021).

$$d_n = \sum_{m=0}^{N-1} r_m e^{-(\frac{2j\pi nm}{N})} \qquad for\,, \quad n = 0,1,2, \dots \dots N-1 \tag{3.38}$$

Generally, time domain expression of OFDM is given by

$$X_{OFDM} = \frac{1}{N}\sum_{K=0}^{K-1} x_k \times \prod(t) \times e^{-j2\pi f_k t} \qquad for, n = 0,1,2, \dots . N-1 \tag{3.39}$$

where x_k signifies the complex symbols that originate from a specific constellation, $\prod(t)$ is the rectangular waveform filter, and *N* is the number of subcarriers. These data symbols are changed to *N* streams, which correspond to subcarrier frequencies using serial to parallel convertor

Then, it travels through IFFT to form time sequence of the streams. In the OFDM signal, the complex values modulating subcarriers in each symbol period are statistically independent of each other, which are orthogonal. Orthogonality of subcarriers prevents intercarrier interference (Kassaw, 2019). At transmission, a cyclic prefix is added, and at reception, it is deleted. It is employed to prevent interference between distinct symbols.

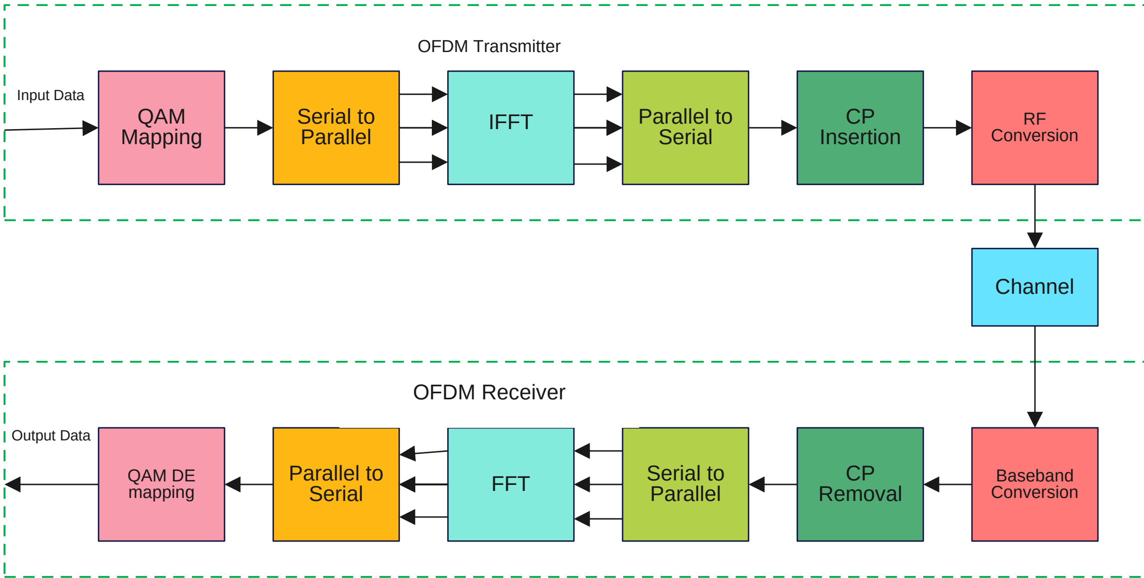

Figure 3.6 OFDM Block diagram

3.6 PHYDYAS filter

The PHYDYAS filter is designed for the European project on cognitive radio and dynamic spectrum access on the physical layer. (A. Viholainen, M. Bellanger, n.d.). It was introduced by Bellanger in (Bellanger, 2001). Based on frequency sampling, it has the advantage of being a closed-form example with a small number of adjustable design parameters. First, using the interpolation formula of the expected frequency response samples $G(k)$, which are continuously moved apart at the frequency points $f_k = \frac{k}{OT}$, where T is the symbol period and O is the overlapping factor, the continuous frequency response $G(f)$ is derived. That is ;

$$G(f) = \sum_k G_k \frac{\sin(\pi(OTf - k))}{\pi(OTf - k)} \tag{3.40}$$

Then, the prototype filter continuous impulse response is obtained by taking $G(f)$ the inverse Fourier transform, which resulting in:

$$g(t) = \sum_k G_k e^{j2\pi\frac{kt}{OT}} \tag{3.41}$$

The frequency coefficients $G(k)$, are chosen in accordance with the Nyquist theory and are upgraded to provide the highest frequency selectivity and minimize the overall interference that results from the filter bank structure for the PHYDYAS prototype filter. The overlapping factor is chosen to be O=4(A. Viholainen, T. Ihalainen, T. Hidalgo Stitz, M. Renfors, 2009). Thus, for the PHYDYAS filter, the frequency coefficients G_K selected are shown by .

$$G_0 = 1, G_1 = 0.971960, G_2 = \frac{1}{\sqrt{2}}, G_3 = \sqrt{1 - G_1^2} = 0.235147 \ , \quad G_k = 0, for\ k > 3\ and\ G_k = G_{-k}, for\ k < 3 \tag{3.42}$$

Therefore, the time-continuous impulse response of the PHYDYAS prototype filter is given by:

$$g(t) = 1 + 2\sum_{k=1}^{O-1} G_k cos\left(2\pi \frac{kt}{OT}\right), \qquad for\ |t| \leq OT \tag{3.43}$$

where G_k, $k \in \{1, 2, ..., O - 1\}$, are given in (3.16), for an overlapping factor of O = 4. The discrete-time prototype filter with *OM* length is gained by sampling $g(t)$ as shown follows:

$$g(m) = g(mT_s) = 1 + 2\sum_{k=1}^{O-1} G_k cos\left(2\pi \frac{km}{OM}\right), \ m = 0,1 \dots \dots OM - 1 \tag{3.44}$$

3.7 Hermite filter

A possible prototype filter for FBMC-QAM is based on Hermite polynomials $H_n(.)$, as proposed in (C.Daniel, Arajo, Taras Maksymyuk, Andr L. F. de Almeida1, Tarcisio Maciel1, Joo C. M. Mota1, n.d.):

$$P(t) = \frac{1}{\sqrt{T_0}}\ e^{-2\pi(\frac{1}{T_0})^{\ 2}} \sum_{i=\{0,4,8,12,16,20\}} a_i H_i(2\sqrt{\pi}\frac{t}{T_0}) \tag{3.45}$$

For which the coefficients can be found to be

$$\begin{aligned} a_0 &= 1.412692577 & a_{12} &= -2.2611.10^{-9} \\ a_4 &= -3.0145.10^{-3} & a_{16} &= -4.4570.10^{-15} \\ a_8 &= -8.8041.10^{-6} & a_{20} &= -1.88633.10^{-15} \end{aligned} \tag{3.46}$$

This leads to the following properties

$$\text{Orthogonality:} \quad T = T_0; \quad F = \frac{2}{T_0} \quad \rightarrow \quad TF = 2$$
$$\text{Localization:} \quad \sigma_t = 0.2015\, T_0 \ \ ; \quad \sigma_f = 0.403/\, T_0 \tag{3.47}$$

Orthogonality is seen with a time spacing of $T = T_0$ and a frequency spacing of $F = 2/T_0$. Compared to OFDM, the frequency localization is significantly better. The Hermite pulse has the same shape in time and frequency, allowing to leverage symmetries.

Furthermore, it is based on a Gaussian function and therefore has a good joint time-frequency localization of $\sigma_t \sigma_f \geq 1.02\, x \frac{1}{4\pi} \approx 0.08$, almost as good as the bound of $\sigma_t \sigma_f \geq \frac{1}{4\pi} \approx 0.08$, making it robust to doubly-selective fading channels.

3.8 Channel Estimation and Equalization

As is widely known, wireless channels have a significant impact on system performance. When there is reliable channel information, the FBMC/QAM systems perform effectively. Thus, in FBMC/QAM systems, channel equalization and estimation play a crucial role. In contrast to OFDM systems, the orthogonality constraint of the FBMC/QAM systems only holds in the real-number field, which results in intrinsic imaginary interference to real sent symbols at the receiver. Because the intrinsic imaginary interference in FBMC/QAM systems must be assumed for the channel estimate patterns, the traditional channel estimation techniques used in OFDM systems cannot be simply applied to QAM/FBMC systems. Channel estimate for the FBMC/QAM systems can now be divided into two groups. These are time-domain channel estimation (Signal & Processing, 2009) and channel estimation in frequency-domain (Nissel, 2016) . In FBMC/OQAM systems, which are comparable to OFDM systems, single-tap equalizers can be used for channel equalization. The frequency domain channel estimation techniques are quite straightforward. However, frequency domain channel estimation approaches are only effective for modest channel delay spread in FBMC/OQAM systems. When the channel delay spread is relatively big, the performance of frequency-domain channel estimation approaches significantly deteriorates. To address this issue, time-domain channel estimating approaches are projected to perform well even for huge channel delay spreads. Regarding the equalization, it is not ideal to use basic single-tap equalizers for the large channel delay spread

3.9 Channel Estimation

Channel estimation, which involves assessing the characteristics of the communication channel between the transmitter and the receiver, is a crucial process in wireless communication systems. The channel estimating approach aims to determine the channel response, which describes how the signal moves across the channel and is affected by various impairments such as multipath propagation, fading, and interference. OFDM is widely used in communication systems to reduce frequency-selective fading in wireless networks. In these channels, the channel itself has an impact on the received signal. It becomes vital to assess and adjust for the channel effects of the receiver in order to efficiently retrieve the broadcast symbols. For accurate channel mapping, the transmitter and the receiver use the time frequency coordinates and values that they already know. Usually, to do this, particular symbols known as pilots are used. (Hussein et al., 2023).

3.9.1.1 Minimum Mean Square Error (MMSE) Estimation

MMSE estimation takes into account both the noise and the received pilot symbols to minimize the mean square error between the estimated and channel responses. It is more accurate than LS estimation since it considers the statistical characteristics of the noise and the channel. However, in practice, it might not always be possible to obtain the channel and noise information needed for MMSE estimation.

$$\tilde{h}_i\,[k] = \tilde{h}_{initial\;i}\,[-21], \tilde{h}_{initial\;i}\,[k], \ldots \tilde{h}_{initial\;i}\,[21]\,;\; k \in N_d \tag{3.48}$$

3.9.1.2 Least Squares (LS) Estimation

A popular and simple method for channel estimation is LS estimation. The mean square error between the estimated symbols and the received pilot symbols is minimized. Although LS estimation is easily computed, noise and interference may cause it to become sensitive. For pilot-based channel estimation, least squares (LS) estimation is a common method since it provides respectable performance with moderate complexity. The channel least squares estimator's objective is to minimize the squared difference between the sent and received signals (Hussein et al., 2023). The least square (LS) channel estimation is a basic solution used in IEEE 802.11p. It employs two received long preambles denoted as $y_1^{(p)}[k]\ and\ y_2^{(p)}[k]$ to estimate the channel gain as follows:

$$\tilde{h}_{LS}[k] = \frac{y_1^{(p)}[k] + y_2^{(p)}[k]}{2p[k]} \tag{3.49}$$

employing the LS estimation without any channel tracking will significantly degrade the performance under mobility conditions. where $\tilde{h}_{LS}[k]$ is the estimated channel at the k-th subcarrier; this estimate ignores the time variations of the channel and its accuracy decreases with the increase of the index i of the OFDM symbol. where $p[k]$ is the predefined frequency domain symbol transmitted on the k-th subcarrier of the long training preamble.

3.9.1.3 Spectral Temporal Averaging (STA)

The spectral temporal averaging (STA) scheme estimates the channel by averaging time and frequency. It can provide better channel estimates in low signal-to-noise ratio (SNR) regions because to the predetermined time and frequency averaging window size, but significant performance loss occurs in high SNR regions. (Gizzini et al., 2020). An improved equalization system called the STA scheme has been presented to address the issue of dynamic channel variations in vehicular communications scheme (J. A. Fernandez, K. Borries, L. Cheng, B. V. K. Vijaya Kumar, D. D. Stancil, 2012). Using data symbol decisions to estimate the channel at data subcarriers while accounting for the time and frequency correlation between consecutive received FBMC symbols, STA constantly updates the channel estimate.

$$\tilde{h}_{FD\ i}\,[k'] = \sum_{\lambda=-\beta}^{\lambda=\beta} \omega_\lambda\, \tilde{h}_{initial\ i}\,[k+\lambda], \omega_\lambda = \frac{1}{2\beta+1} \quad (3.50)$$

where k' = [3,.., Kon − 2], ω_λ is a set of weighting factors with unit sum, and 2β + 1 denotes the average number of subcarriers. The frequency domain averaging technique excludes the subcarriers at both edges of the received FBMC symbols (positions = 1, 2, 51, 52). Lastly, time averaging is carried out by STA to determine the ultimate STA channel estimate, which is as follows:

$$\tilde{h}_{STA\,(i)}\,[k] = \left(1-\frac{1}{\alpha}\right)\tilde{h}_{STA\,(i-1)}\,[k] + \frac{1}{\alpha}\tilde{h}_{FD\ i}\,[k'] \quad (3.51)$$

In order to reduce demapping error and increase estimation accuracy, time and frequency averaging is employed (J. A. Fernandez, K. Borries, L. Cheng, B. V. K. Vijaya Kumar, D. D. Stancil, 2012). The next received FBMC symbol is then equalized using this final channel estimate, and so on until all of the symbols in the packet are equalized. The characteristics of vehicle channels determine the values of α and β. As per the analysis conducted in (J. A. Fernandez, K. Borries, L. Cheng, B. V. K. Vijaya Kumar, D. D. Stancil, 2012), it is possible to attain noteworthy accuracy by modifying these values based on the understanding of the vehicular channel environment. Generally speaking, a slowly shifting channel is better suited for a large value of α. Furthermore, if α and β are made extremely big, too many subcarriers (in frequency) or symbols (in time) will be averaged, blurring the estimated channel and making the final channel estimate erroneous in vehicular communications where the channel varies very quickly. However, in actual case scenarios, it is practically extremely difficult to get such information since, aside from the noise influence, the vehicular channel's behavior cannot be correctly predicted. Consequently, it is possible to appropriately select fixed values for these parameters and still have an acceptable performance degradation.

3.9.1.4 Constructed Data Pilots (CDP) Scheme

The built data pilots (CDP) approach estimates the channel effectively, especially in high SNR regions, but it is still unable to deliver an acceptable error performance in high mobility scenarios due to the high correlation between the received symbols (Gizzini et al., 2020). The CDP estimation scheme (Z. Zhao, X. Cheng, M. Wen, B. Jiao, 2013)has been proposed to alleviate the effects of demapping errors when updating the channel estimate. The high time correlation of the channel response between two neighboring FBMC symbols is the foundation of the CDP system. The first three steps needed for the initial channel estimate process are shared by this approach. Given the strong time correlation between successively received OFDM symbols, CDP suggests two distinct stages in place of the time and frequency averaging carried out in STA. After calculating the initial channel estimation from (I. Goodfellow, Y. Bengio, 2016), the previously received OFDM symbol is equalized by $\tilde{h}_{initial\ i}\,[k] and\ \tilde{h}_{CDP\ i-1}\,[k]$ respectively as follows:

$$\widetilde{y'}_{eq\ i-1}\,[k] = \frac{y_{i-1}[k]}{\tilde{h}_{initial\ i}\,[k]} \tag{3.52}$$

$$\widetilde{y''}_{eq\ i-1}\,[k] = \frac{y_{i-1}[k]}{\tilde{h}_{CDP\ i-1}\,[k]} \tag{3.53}$$

Then, the obtained $\widetilde{y'}_{eq\ i-1}\,[k]$ and $\widetilde{y''}_{eq\ i-1}\,[k]$ are demapped into $\widetilde{d'}_{eq\ i-1}\,[k]$ and $\widetilde{d''}_{eq\ i-1}\,[k]$ respectively according to the used constellation. Finally, CDP applies a comparison step where the final $\tilde{h}_{CDP\ i}\,[k]$ is obtained as:

$$\tilde{h}_{CDP\ i}\,[k] = \begin{Bmatrix} \tilde{h}_{CDP\ i-1}\,[k] & , & \widetilde{d'}_{i-1}\,[k] \neq \widetilde{d''}_{i-1}\,[k] \\ \tilde{h}_{initial\ i}\,[k] & , & \widetilde{d'}_{i-1}\,[k] = \widetilde{d''}_{i-1}\,[k] \end{Bmatrix} \tag{3.54}$$

The case where $\widetilde{d'}_{i-1}\,[k] \neq \widetilde{d''}_{i-1}\,[k]$, indicates that $\tilde{h}_{initial\ i}\,[k]$ is unreliable, and thus, the previous channel estimate is used. Stated differently, the demapping results of the previous received FBMC symbol when it is equalized by $\tilde{h}_{initial\ i}\,[k]$ and $\tilde{h}_{CDP\ i-1}\,[k]$ should be identical due to the high time correlation between two received successive FBMC symbols for $\tilde{h}_{initial\ i}\,[k]$ to be regarded as a reliable channel estimate. Performance degradation occurs in this channel update process in high mobility environments, especially for high order modulation schemes like 16QAM and 64QAM.

3.10 Channel Equalization in Doubly Selective Channels

Although channel equalization techniques might increase computing complexity, they can also improve performance. Instead of just using nearby time symbols, the n-tap MMSE equalizer incorporates nearby subcarriers into the equalization process (D. S. Waldhauser, L. G. Baltar, n.d.), (Louveaux, 2009) , (L. Marijanovic, S. Schwarz, n.d.). Subsequently, more elaborate equalization techniques can increase performance at the expense of complexity. The MMSE equalizer derivation for doubly selective channels is as follows.

$$y = Dx + n \tag{3.55}$$

where transmission matrix *D* helps to keep the notation compact and is defined as

$$D = Q^H HG \tag{3.56}$$

Note that $n \sim \mathrm{CN}(0, \mathrm{Pn}\ \mathrm{QHQ})$ denotes the Gaussian noise. A conventional (complex-valued) MMSE equalizer could be used to estimate the transmitted data symbols x in (3.57), but this approach is not effective because it would introduce imaginary interference into the minimization problem, resulting in large detection errors; instead, the real and imaginary parts are stacked in a large vector, as proposed in (D. S. Waldhauser, L. G. Baltar, n.d.). The full block MMSE equalization of *y*, as (3.55), can then be calculated by:

$$\hat{\mathbf{x}} = \begin{bmatrix} \Re\{\mathrm{D}\} \\ \Im\{\mathrm{D}\} \end{bmatrix}^{\top} \left(\begin{bmatrix} \Re\{\mathrm{D}\} \\ \Im\{\mathrm{D}\} \end{bmatrix} \begin{bmatrix} \Re\{\mathrm{D}\} \\ \Im\{\mathrm{D}\} \end{bmatrix}^{\top} + \Psi \right)^{-1} \begin{bmatrix} \Re\{\mathrm{y}\} \\ \Im\{\mathrm{y}\} \end{bmatrix}, \tag{3.57}$$

with noise matrix Ψ given by

$$\mathbf{\Psi} = \frac{P_{\mathrm{n}}}{2} \begin{bmatrix} \mathcal{R}\{\mathrm{Q^H Q}\} & -\Im\{\mathrm{Q^H Q}\} \\ \Im\{\mathrm{Q^H Q}\} & \Re\{\mathrm{Q^H Q}\} \end{bmatrix}. \tag{3.58}$$

Keep in mind that the eigenvalues of the matrix to be inverted in Eq. (3.57) are typically incredibly small. This is a result of the compressing of time and frequency. Unlike many other systems, noise matrix Ψ does not ensure full rank since it shares exactly the same structure as D in the case of an AWGN channel. As a result, solving Eq. (3.57) is extremely difficult numerically and necessitates, among other things, an eigen decomposition together with implicitly putting small eigenvalues to zero in MATLAB using the pseudo inverse. However, the complete block MMSE equalization has two more major issues: Its great computational complexity is the first drawback. A matrix of dimension *2LK×2LK*, which is too big for most real-world applications, must be inverted. Second, because equalization cannot occur until all symbols are received, a significant delay is imposed. Consequently, an n-tap MMSE equalizer that only has a small number of nearby symbols. By spliting the transmission model of Eq. (3.55) to:

$$\mathbf{y}_{\mathcal{S}} = \mathbf{D}_{\mathcal{S}}\mathbf{x}_{\mathcal{S}} + \mathbf{D}_{\mathcal{S},\mathcal{R}}\mathbf{x}_{\mathcal{R}} + \mathbf{n}_{\mathcal{S}} \tag{3.59}$$

Here, $\mathbf{y}_{\mathcal{S}} \in C^{|s|x2}$ is a subvector of $\mathbf{y}$ with $\mathcal{S}$ representing the considered subblock, that is, certain time-frequency position. For example, a subblock vector of size $\mathcal{S} = 5$ (5-tap) can be written as:

$$\mathbf{y}_{\mathcal{S}} = [\mathbf{y}_{l,k-2}\ \ \mathbf{y}_{l,k-1}\ \ \mathbf{y}_{l,k}\ \ \mathbf{y}_{l,k+1}\ \ \ \ \mathbf{y}_{l,k+2}]^{T} \tag{3.60}$$

This particular subblock was utilized in and only contains nearby symbols at that point in time, ignoring nearby subcarriers(D. S. Waldhauser, L. G. Baltar, n.d.). This is frequently not the best option, particularly in situations involving high velocities and for particular prototype filters.

My considered subblock vector, on the other hand, can be expressed by

$$\mathbf{y}_{\mathcal{S}} = [\mathbf{y}_{l,k-1}\ \ \mathbf{y}_{l-1,k}\ \ \mathbf{y}_{l,k}\ \ \mathbf{y}_{l+1,k}\ \ \ \ \mathbf{y}_{l,k+1}]^{T} \tag{3.61}$$

Vector $\mathbf{x}_{\mathcal{S}} = R^{|s|x1}$ in (3.61) represents the transmitted data symbols of the considered subblock, while $\mathbf{x}_{R} = R^{|s|x1}$ represents all other transmitted data symbols relevant for $\mathbf{y}_{\mathcal{S}}$. Only a few symbols outside the subblock have a significant contribution on $\mathbf{y}_{\mathcal{S}}$, so that usually $|\mathcal{R}| < < LK - |\mathcal{S}|$. |. The matrices $\mathbf{D}_{\mathcal{S}} \in \mathbb{C}^{|\mathcal{S}|\times|\mathcal{S}|}$ and $\mathbf{D}_{\mathcal{S},\mathcal{R}} \in \mathbb{C}^{|\mathcal{S}|\times|\mathcal{R}|}$correspond to the correct elements of $\mathbf{D}$, so that Eq. (3.61) satisfies Eq. (3.55). Similar to Eq. (3.57), the $|\mathcal{S}|$-tap MMSE equalization of Eq. (3.59) becomes

$$\hat{\mathbf{x}}_{\mathcal{S}} = \begin{bmatrix}\Re\{\mathbf{D}_{\mathcal{S}}\}\\ \Im\{\mathbf{D}_{\mathcal{S}}\}\end{bmatrix}^{\top} \left(\Delta_{\mathcal{S}} + \Delta_{\mathcal{S},\mathcal{R}} + \Psi_{\mathcal{S}}\right)^{-1} \begin{bmatrix}\Re\{\mathbf{y}_{\mathcal{S}}\}\\ \Im\{\mathbf{y}_{\mathcal{S}}\}\end{bmatrix} \tag{3.62}$$

with

$$\Delta_{\mathcal{S}} = \begin{bmatrix}\Re\{\mathbf{D}_{\mathcal{S}}\}\\ \Im\{\mathbf{D}_{\mathcal{S}}\}\end{bmatrix} \begin{bmatrix}\Re\{\mathbf{D}_{\mathcal{S}}\}\\ \Im\{\mathbf{D}_{\mathcal{S}}\}\end{bmatrix}^{\top} \tag{3.63}$$

$$\Delta_{\mathcal{S}} = \begin{bmatrix}\Re\{\mathbf{D}_{\mathcal{S},\mathcal{R}}\}\\ \Im\{\mathbf{D}_{\mathcal{S},\mathcal{R}}\}\end{bmatrix} \begin{bmatrix}\Re\{\mathbf{D}_{\mathcal{S},\mathcal{R}}\}\\ \Im\{\mathbf{D}_{\mathcal{S},\mathcal{R}}\}\end{bmatrix}^{\top} \tag{3.64}$$

Noise matrix $\Psi_{\mathcal{S}} \in \mathbb{C}^{2|\mathcal{S}|\times 2|\mathcal{S}|}$ in Eq. (3.58) is given by the submatrix of $\Psi \in \mathbb{C}^{2LK\times 2LK}$, corresponding to the correct elements. Note that $\hat{\mathbf{x}}_{\mathcal{S}}$ in Eq. (3.62) delivers in total |S| estimates.

The remaining elements are discarded. Thus, the equalization requires in total LK matrix inversions of size $2|\mathcal{S}| \times 2|\mathcal{S}|$. The computational complexity is usually lower then for the full block MMSE equalizer but still relatively high.

3.11 FBMC-QAM Bit Error Probability in Doubly-Selective Channels

Comparing various modulation techniques in time-variant multipath propagation—that is, time- and frequency-selectivity, or double selectivity is of particular interest. The Bit Error Probability is a crucial parameter for the comparison (BEP). The FBMC-QAM BEP in doubly-selective fading channels is computed by a concise mathematical derivation. Perfect channel knowledge at the receiver, a Rayleigh fading channel, and the selection of data symbols from a quadrature amplitude Symbols are often sent across a rectangular time-frequency grid in multi-carrier transmissions. By denoting the transmit data symbol at subcarrier position l and time-position k by $x_{l,k} \in A$ with A denoting the symbol alphabet. The transmitted signal $S(t)$, consisting of L subcarriers and K time-symbols, then

$$S(t) = \sum_{k=1}^{K} \sum_{l=1}^{L} g_{l,k}(t) x_{l,k}) \tag{3.65}$$

with the basis pulses $g_{l,k}(t)$ are, essentially, time and frequency shifted versions of the prototype filter *p(t):*

$$g_{l,k}(t) = P(t - kT) e^{j2\pi IF(t-kT)} e^{j\theta_{l,k}} \tag{3.66}$$

Observe that the spectral efficiency is determined by the time separation T and the frequency spacing F. Sadly, the Balian-low theorem states that it is impossible to identify basis pulses with a time-frequency spacing of TF = 1, localization in both time and frequency, and orthogonality (X. Zhang, M. Jia, L. Chen, J. Ma, 2015) . It is necessary to give up at least one of these desired characteristics. P(t) is a rectangular function in pure OFDM, which defies frequency-localization. Furthermore, to increase resilience in frequency-selective channels, a Cyclic Prefix (CP) is frequently added to OFDM, which lowers the spectral efficiency *(TF = 1 + TCPF > 1).* In contrast, FBMC typically uses a prototype filter, *p(t),* that is localized in both frequency and time. For *TF = 2,* this prototype filter is orthogonal. After that, a factor of two is applied to both the time and frequency spacing, resulting in *TF = 0.5*. This results in interference, but by choosing $\theta_{l,k} = \pi \times 2(l + k)$ for the phase shift, the interference is moved to the purely imaginary domain. Only real valued signals may be communicated due to imaginary interference, requiring two real valued symbols to convey one complex symbol. This results in an information rate equal to that of OFDM without CP, or TF = 1. By substituting the less stringent real orthogonality criteria for the complex orthogonality condition, FBMC thereby satisfies the Balian-low theorem. An analytical study can be made simpler by using a time discrete model of our transmission system. By writing the sampled transmit signal $S(t)$ in a vector $S \in \mathbb{C}^{N\times 1}$, we can reformulate Eq. (3.65) by

$$s = Gx \tag{3.67}$$

with

$$G = [g_{1,1}\ \ g_{2,1}\ \ g_{L,1}\quad g_{1,2} \cdots\ \ g_{L,K}] \tag{3.68}$$

$$x = [x_{1,1}\ \ x_{2,1}\ \ x_{L,1}\quad x_{1,2} \ldots.\ \ x]^{\,T} \tag{3.69}$$

Vector $g_{l,k} \in \mathbb{C}^{N\times 1}$ represents the sampled basis pulses of (2) and builds the transmit matrix $G \in \mathbb{C}^{N\times LK}$ while $x \in \mathbb{C}^{LK\times 1}$ stacks all the transmitted data symbols in a large vector. By denoting the receive matrix by $Q = [q_{1,1} \ldots \ldots \ldots \ldots q_{L,K}\ \in \mathbb{C}^{N\times LK}]$ which is similarly defined as the transmit matrix, but a different prototype filter *p(t)* might be used. With a time-variant convolution matrix $H \in \mathbb{C}^{N\times N}$ the whole transmission system can then be expressed as:

$$y = Q^H HGx + n \tag{3.70}$$

Where $y = [y_{1,1}\ \ldots \ldots \ldots\ \ y_{L,K}]^{\,T} \in \mathbb{C}^{LK\times 1}$ represents the received symbols and $n \sim \mathbb{C}N(0, P_n Q^H Q)$ the Gaussian distributed noise. Without loss of generality, we normalize the receive matrix so that

$q_{l,k}^H q_{l,k} = 1$. In FBMC and pure OFDM, we have $Q = G$, while in CP-OFDM the transmit and receive matrix are slightly different, $Q \neq G$. Note that the orthogonality condition of OFDM implies that $Q^H G = I_{LK}$ and the real orthogonality condition of FBMC that $\mathbb{R}\{Q^H G\} = I_{LK}$. In doubly-selective channels, orthogonality no longer holds, leading to interference, described by the off-diagonal elements of $Q^H HG$. The diagonal elements, on the other hand, describe the signal components. To keep the statical investigation simple. By utilizing the Kronecker product $\otimes$ to rewrite Eq. (3.72) for the received symbol

$$y_{l,k} = q_{l,k}^H HGx + n_{l,k} = \left((Gx)^T \otimes q_{l,k}^H\ \right) vec\{H\} + n_{l,k}\big) \tag{3.71}$$

where $vec\{H\}$ denotes the vectorized time-variant convolution matrix. Finally, the estimated data symbols $\tilde{x}_{l,k}$at the receiver are obtained by one-tap equalization, that is,

$$\tilde{x}_{l,k} = \mathrm{Q}\left\{\frac{y_{l,k}}{h_{l,k}}\right\} \tag{3.72}$$

with the relevant diagonal element of $Q^H HG$ denoted by $h_{l,k} = q_{l,k}^H H\, g_{l,k}$ and Q{.}, the quantization operator, or closest neighbor detection. Since the majority of the energy is focused at the diagonal parts of $Q^H HG$, one-tap equalizers function well up to a certain threshold for Signal-to-Noise Ratio (SNR). Moreover, one-tap equalizers correspond to the maximum likelihood symbol recognition as long as the interference is dominated by the (Gaussian) noise, which clarifies why they are so helpful in reality.

To calculate the BEP, By Letting y and h be zero mean, correlated, complex valued, Gaussian random variables, then the Cumulative Distribution Function (CDF) of the complex Gaussian ratio $\frac{y}{h}$ given by

$$\mathrm{CDF}_{\frac{y}{h}}(z_\mathrm{R}, z_\mathrm{I}) = \Pr\left\{\left(\Re\left\{\frac{y}{h}\right\} < z_\mathrm{R}\right) \wedge \left(\Im\left\{\frac{y}{h}\right\} < z_\mathrm{I}\right)\right\}$$

$$= \frac{1}{4} + \frac{(z_\mathrm{R} - \Re\{\alpha\})\left(2\tan^{-1}\left(\frac{z_1 - \Im\{\alpha\}}{\sqrt{(z_\mathrm{R} - \Re\{\alpha\})^2 + \beta - |\alpha|^2}}\right) + \pi\right)}{4\pi\sqrt{(z_\mathrm{R} - \Re\{\alpha\})^2 + \beta - |\alpha|^2}} + + \frac{(z_\mathrm{I} - \Im\{\alpha\})\left(2\tan^{-1}\left(\frac{z_\mathrm{R} - \Re\{\alpha\}}{\sqrt{(z_1 - \Im\{\alpha\})^2 + \beta - |\alpha|^2}}\right) + \pi\right)}{4\pi\sqrt{(z_\mathrm{I} - \mathfrak{Y}\{\alpha\})^2 + \beta - |\alpha|^2}} \tag{3.73}$$

With

$$\alpha = \frac{\mathrm{E}\{\mathrm{yh}*\}}{\mathrm{E}\{|h|^2\}}\ and\ \beta = \frac{\mathrm{E}\{\mathrm{yh}*\}}{\mathrm{E}\{|h|^2\}} \tag{3.74}$$

By considering $y_{l,k}$ be Gaussian distributed and utilizing Eq. 3.73 the required expectations in Eq. (3.76), conditioned on x, is calculated as follows

$$\mathbb{E}\left\{\left|y_{l,k}\right|^2 \mid \mathbf{x}\right\} = \mathbf{x}^\top\left(\mathbf{G}^\top \otimes \mathbf{q}_{l,k}^\mathrm{H}\right)\mathbf{R}_{\mathrm{vec}\,\{\mathbf{H}\}}\left(\mathbf{G}^\top \otimes \mathbf{q}_{l,k}^\mathrm{H}\right)^\mathrm{H}\mathbf{x}^* + P_\mathrm{n} \tag{3.75}$$

$$\mathbb{E}\left\{\left|h_{l,k}\right|^2\right\} = \left(\mathbf{g}_{l,k}^\top \otimes \mathbf{q}_{l,k}^\mathrm{H}\right)\mathbf{R}_{\mathrm{vec}\,\{\mathbf{H}\}}\left(\mathbf{g}_{l,k}^\top \otimes \mathbf{q}_{l,k}^\mathrm{H}\right)^\mathrm{H} \tag{3.76}$$

$$\mathbb{E}\left\{\left|h_{l,k}\right|^2\right\} = \left(\mathbf{g}_{l,k}^\top \otimes \mathbf{q}_{l,k}^\mathrm{H}\right)\mathbf{R}_{\mathrm{vec}\,\{\mathbf{H}\}}\left(\mathbf{g}_{l,k}^\top \otimes \mathbf{q}_{l,k}^\mathrm{H}\right)^\mathrm{H} \tag{3.77}$$

in which $\mathbf{R}_{\mathrm{vec}\,\{\mathbf{H}\}} = \mathbb{E}\{\mathrm{vec}\{\mathrm{H}\}\mathrm{vec}\{H\}^H$ represents the correlation matrix of the vectorized time-variant convolution matrix and depends on the underlying power delay profile and the Doppler spectral density. We normalize the channel so that it has unit power, that is, the taps of the power delay profile sum up to one. Combining Eq. (3.77) to (3.79) allows us to express the CDF, conditioned on x, of our transmission system in Eq. (3.74), $CDF = \frac{y_{l,k}}{h_{l,k}}(Z_{R,}Z_I|X)$. To calculate the overall BEP, however, we need the CDF conditioned solely on $x_{l,k}$. With a permutation matrix **P** we split the transmitted symbols **x** into interfering symbol $x_{l,k} \in A^{(LK-1)x1}$ and the symbol of interest, $x_{l,k}$, according to $X = P[X_{I\,l,k}^T , x_{l,k}]^T$. The required CDF can then be calculated by the law of total probability:

$$\mathrm{CDF}_{y_{l,k}/h_{l,k}}\left(z_{\mathrm{R}}, z_{\mathrm{I}} \mid x_{l,k}\right) = \frac{1}{M} \sum_{\mathbf{x}_{l,k} \in \mathcal{A}^{LK-1}} \mathrm{CDF}_{y_{l,k}/h_{l,k}}\left(z_{\mathrm{R}}, z_{\mathrm{I}} \mid \mathbf{x}_{\mathrm{I}_{l,k}}, x_{l,k}\right) \tag{3.78}$$

With $M = \mathcal{A}^{LK-1}$ denoting the cardinality. Equation 3.80 is required to model the interference influence correctly. Also , the transmit symbol $x_{l,k}$, given by:

$$\mathrm{BEP}_{l,k} = \frac{1}{\log_2 |\mathcal{A}|} \sum_{p=1}^{\log_2 |\mathcal{P}|} \frac{1}{|\mathcal{A}|} \sum_{j=1}^{|\mathcal{H}|} \sum_{a_i \in \mathcal{E}_j^p} \Pr\left\{\hat{x}_{l,k} = a_i \mid x_{l,k} = a_j\right\} \tag{3.79}$$

The symbol alphabet is described as Set $\mathcal{A} = \{a_1, \dots . a_{|\mathcal{A}|}\}$ and each symbol is mapped to a distinct bit sequence of size $\log_2|\mathcal{A}|$. In contrast, all the elements of $\mathcal{A}$ for which the bit-value at bit-position p ∈ N differs from the matching bit-value of a_j are represented by set $\mathcal{E}_j^p$. Keep in mind that $\mathcal{E}_j^p$has cardinality $\frac{|\mathcal{A}|}{2}$. However, we find compact formulas for the significant particular case of doubly flat Rayleigh fading, i.e., $\mathbf{H} = \bar{h}\mathbf{I}_N$ with $\bar{h} \sim \mathcal{CN}(0,1)$. For OFDM, the required expectations in Eq. (3.77)-(3.79) simplify to

$$\mathbb{E}\left\{\left|y_{l,k}\right|^2 \mid \mathbf{x}\right\} = \left|x_{l,k}\right|^2 + P_n \tag{3.80}$$

$$\mathbb{E}\left\{\left|h_{l,k}\right|^2\right\} = 1 \text{ and } \mathbb{E}\left\{y_{l,k} h_{l,k}^* \mid \mathbf{x}\right\} = x_{l,k} \tag{3.81}$$

, and no longer depend on the surrounding data symbols $x_{l,k}$, simplifying Eq. (3.80). For Gray-coded 4-QAM, symmetries allow us to rewrite Eq. (3.81) by

$$\mathrm{BEP}_{l,k} = \mathrm{CDF}_{yl,k/h_{l,k}}\left(0, \infty \,\middle|\, \sqrt{P_x}\frac{1+\mathrm{j}}{\sqrt{2}}\right) \tag{3.82}$$

which, together leads to:

$$\mathrm{BEP}_{4\mathrm{QAM}} = \frac{1}{2} - \frac{1}{2\sqrt{1 + 2\frac{1}{\mathrm{SNR}}}} \tag{3.83}$$

SNR identical for each transmit symbol. FBMC experiences imaginary interference. However, this does not influence the BEP for a doubly-flat channel, so that Eq. (3.85) also describes the BEP for 2-QAM FBMC. Similar the BEP for 16-QAM is given by:

$$\mathrm{BEP}_{16\mathrm{QAM}} = \frac{1}{2} - \frac{3}{8\sqrt{1 + 10\frac{1}{\mathrm{SNR}}}} - \frac{6}{8\sqrt{9 + 10\frac{1}{\mathrm{SNR}}}} + \frac{5}{8\sqrt{25 + 10\frac{1}{\mathrm{SNR}}}} \tag{3.84}$$

The SNR in Eqs. (3.85) and (3.86) is defined as:

$$\mathrm{SNR} = \frac{P_x^{\mathrm{OFDM}}}{P_n} = \frac{P_x^{\mathrm{FBMC}}}{\frac{1}{2}P_n} \tag{3.85}$$

where $P_n = \mathbb{E}\left\{\left|x_{l,k}\right|^2\right\}$ represents the average data symbol power. For the same bandwidth *FL*, by setting,

$$P_x^{\mathrm{FBMC}} = \frac{1}{2}P_x^{\mathrm{OFDM}} \tag{3.86}$$

As (3.88), implies that the average transmit power

$$P_n = \frac{1}{KT}\int_{-\infty}^{\infty}\mathbb{E}\{|\mathrm{s(t)}|^2\,dt\} \tag{3.87}$$

is the same for OFDM, CP-OFDM and FBMC, allowing a fair comparison. FBMC $\frac{1}{2}$ only experiences half the noise power due to “taking the real part”, which explains the factor of in.

3.12 Proposed system model

The performance metrics of multicarrier modulation such as Bit Error Rate (BER), Signal-to-Noise Ratio (SNR), Mean-Squared-Error (MSE) and throughput are need further improvement to make ready for 5G and beyond technology.

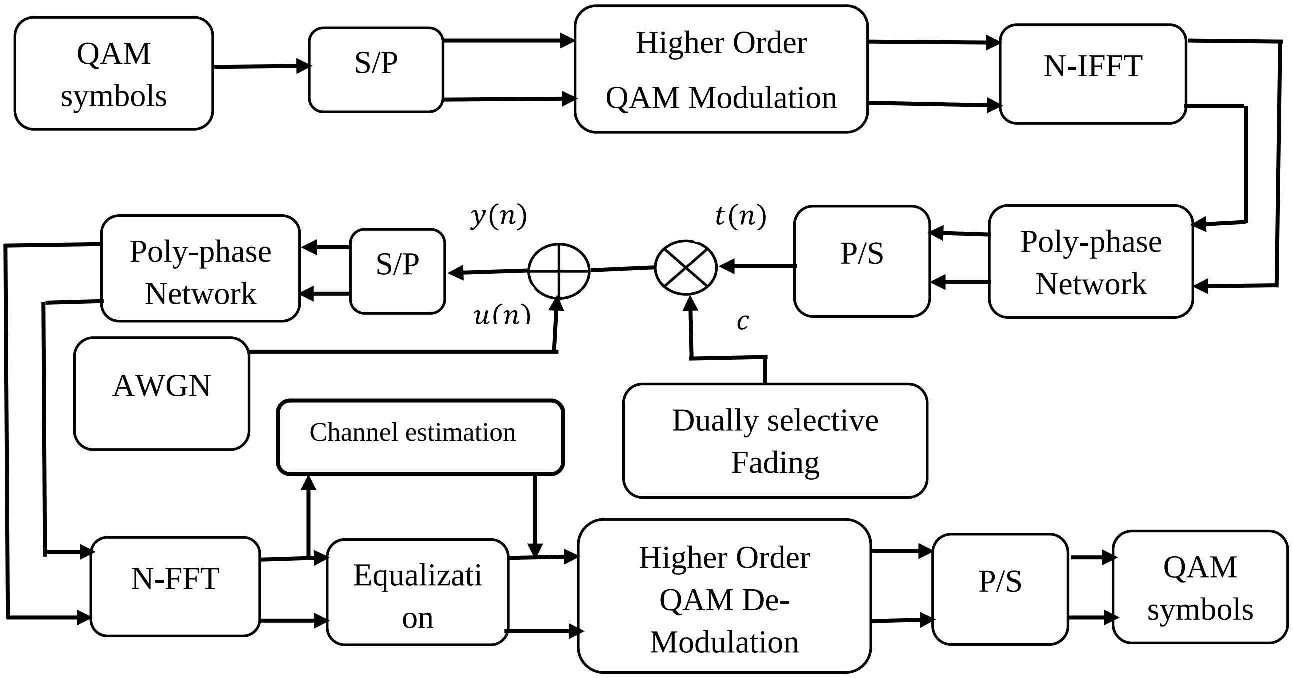

Figure 3.7 Block diagram of proposed system model

In this paper we attempted to examine the advantages of dually selective fading for applications beyond 5G. Dually selective fading contains both time and frequency selective fading. The serial stream from a binary source is transformed into parallel data streams in the higher-order QAM modulator. The conversion to the time domain is done using the IFFT technique. The IFFT's output stream is appropriate for use with the Poly-phase Network (PPN) FIR filter. Synthesis filters are the name for these transmitter-side PPN filters. For transmission, the output of these filters is again transformed into a serial pattern. The signal is split into parallel streams before being transferred via the RF down conversion. The signal is first converted into the frequency domain using the Fast Fourier Transform, which is the analytic filter on the receiver side, known as the PPN. Lastly, higher order QAM is transformed back into QAM, allowing the original data bits to be recovered.

3.12.1 Doubly-selective fading

Doubly selective fading combines the effects of time-selective fading and frequency-selective fading, resulting in a more complex channel environment. It can occur in scenarios where the wireless channel introduces both time-varying characteristics and frequency-dependent effects.

The presence of doubly selective fading poses significant challenges for communication systems. The variations in the channel response across time and frequency can lead to inter-symbol interference (ISI) and inter-carrier interference (ICI), degrading the quality of the received signal and impacting the system's performance.

3.12.2 Inter-carrier interference (ICI)

Inter-carrier interference (ICI) is a commonly recognized issue that negatively affects the quality of Orthogonal Frequency Division Multiplexing (OFDM) transmission. It arises in wireless communication when there are Doppler shifts or frequency-selective fading channels. These wireless channel variations cause different frequency offsets or phase shifts for the subcarriers. Consequently, the orthogonality of the subcarriers is compromised, leading to interference.

3.12.3 Inter-symbol interference (ISI)

Inter-symbol interference (ISI) is a form of distortion of a signal in which one symbol interferes with subsequent symbols. This is an unwanted phenomenon as the previous symbols have a similar effect as noise, thus making the communication less reliable. The spreading of the pulse beyond its allotted time interval causes it to interfere with neigh-boring pulses. ISI is usually caused by multipath propagation or the inherent linear or non-linear frequency response of a communication channel causing successive symbols to blur together. The presence of ISI in the system introduces errors in the decision device at the receiver output. Therefore, in the design of the transmitting and receiving filters, the objective is to minimize the effects of ISI, and thereby deliver the digital data to its destination with the smallest error rate possible.

CHAPTER FOUR

4. RESULTS AND DISCUSSION

In this chapter the simulation results of this thesis work are presented. Simulation results and discussions on the performances comparison of FBMC-QAM, OFDM, UFMC and f-ODDM, the performance comparison between channel estimation technics, different prototype filters performance is compared under doubly selective fading channel are provided.

Table 4.1 Simulation Parameters (Nissel & Rupp, 2017)

No	Simulation Parameter	Type and Value	Remark
1	Modulation	FBMC, OFDM, UFMC, f-OFDM,WOLA-OFDM	
2	Bandwidth	2Mb	
3	Sampling frequency	15.36MHz	
4	No of Cyclic prefix	72	
5	QAM Modulation Order	256,1024	
6	Noise	AWGN	
7	Channel	Double Selective Fading	
8	Prototype filter	PHYDYAS, Hermite, RRC	
9	SNR range	0dB to 30dB	
10	Monte Carlo Repetitions	1000	1000 number of iterations used
11	Number of subcarriers	4	
12	Subcarrier Spacing:	15 kHz	

4.1 Comparison of Different Prototype Filters

The different prototype as PHYDYAS prototype filter, root raised cosine (RRC) filter, Hermite and Rectangular filters frequency and impulse response compared as shown in Fig. 4.1. Compared to the other filters type, PHYDYAS filter offers the best localization in time and frequency. Multicarrier modulation techniques can be affected by the choice of filters, and to achieve better performance with minimum out-of-band emission, a filter with small side lobes is required. An analysis of the power spectral density (PSD) versus normalized frequency for different prototype filters, considering a subcarrier spacing of 15 kHz, 1024 subcarriers, and an overlapping factor of 2, reveals that the Hermite prototype filter provides better performance compared to PHYDYAS, root-raised cosine (RRC), and rectangular prototype filters. Specifically, the Hermite prototype filter exhibits a faster power spectral density decay rate, as can be observed in Figure 4.1. Based on the superior performance of the Hermite prototype filter, it is chosen as the best option to improve the performance of filter bank multicarrier with quadrature amplitude modulation (FBMC-QAM) systems. In comparison, the root-raised cosine (RRC) filter response continues in the time domain, which makes it a less suitable choice for FBMC systems. In this context, the quality of the filter bank system is largely contingent on the properties of the prototype filter used.

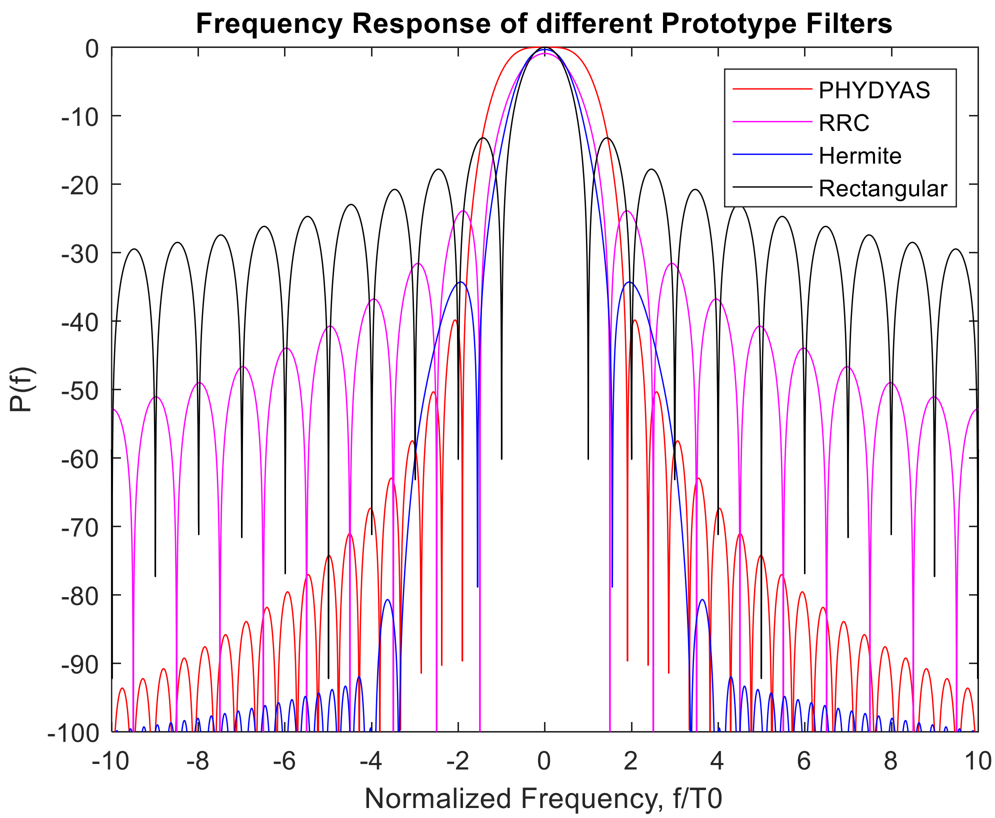

Figure 4.1 Frequency response of different prototype filters (sub carrier spacing 15KHz, L=1024, Overlapping factor =2)

4.2 Effect of Overlapping Factor on the Power Spectral Density

Figure 4.2 below depicted an increase of overlapping factor provides a faster delay of sidelobes. As the overlapping factor is increased from 2 to 4, the side lobe energy of the filter decays at a faster rate. This is crucial for reducing the out-of-band (OOB) emission, which in turn allows the system to support the coexistence of multiple services. However, this improvement in performance comes with a trade-off, as the complexity of the system also increases with the higher overlapping factor.

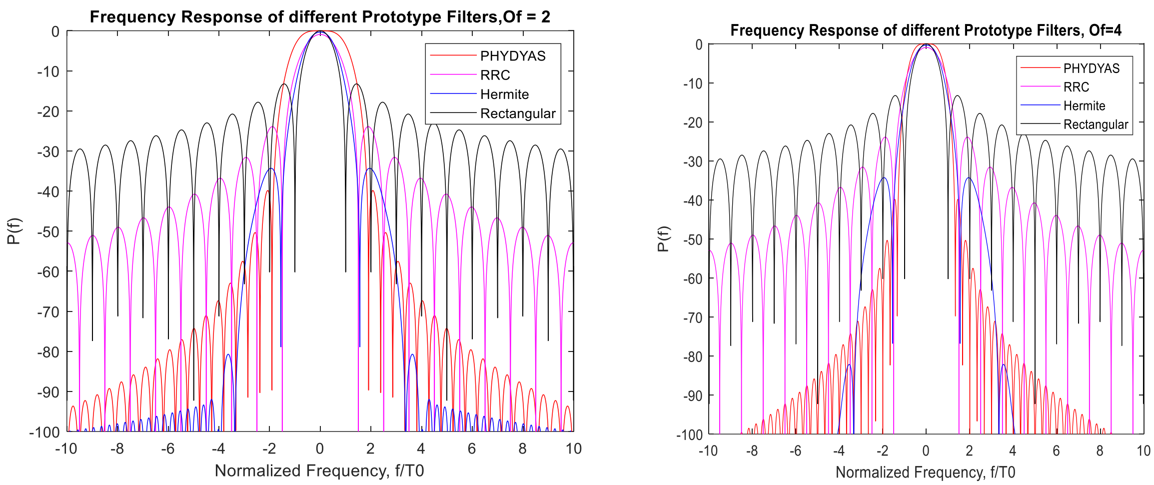

Figure 4.2 The effect of overlapping factor on out of band emission

4.3 Comparison of Normalized Frequency Versus Power Spectral Density of FBMC

Figure 4.3 depicted the comparison of Power spectral density versus normalized frequency for FBMC and OFDM, windowing and filtering signals. We can see that FBMC-QAM is more spectrally efficient and has much improved spectral properties than OFDM, OFDM has a very large sideband when compared to FBMC. The sideband of FBMC can be further suppressed by increasing the number of filter coefficients. However, this increase in filter coefficients leads to higher complexity at both the transmitter and receiver. Alternative OFDM-based techniques, such as windowing (WOLA) and filtering (UFMC, f-OFDM), can also be used to improve the spectral properties of cyclic prefix OFDM (CP-OFDM). Despite these improvements, FBMC still maintains the advantage of maximum symbol density (TF = 1, complex), and generally outperforms these other techniques.

Low out-of-band (OOB) emissions are required to ensure a relatively small guard band between different use cases. FBMC has a maximum symbol density of TF = 1, while in OFDM-based schemes, the symbol density is lower (TF > 1), further worsening the spectral efficiency.

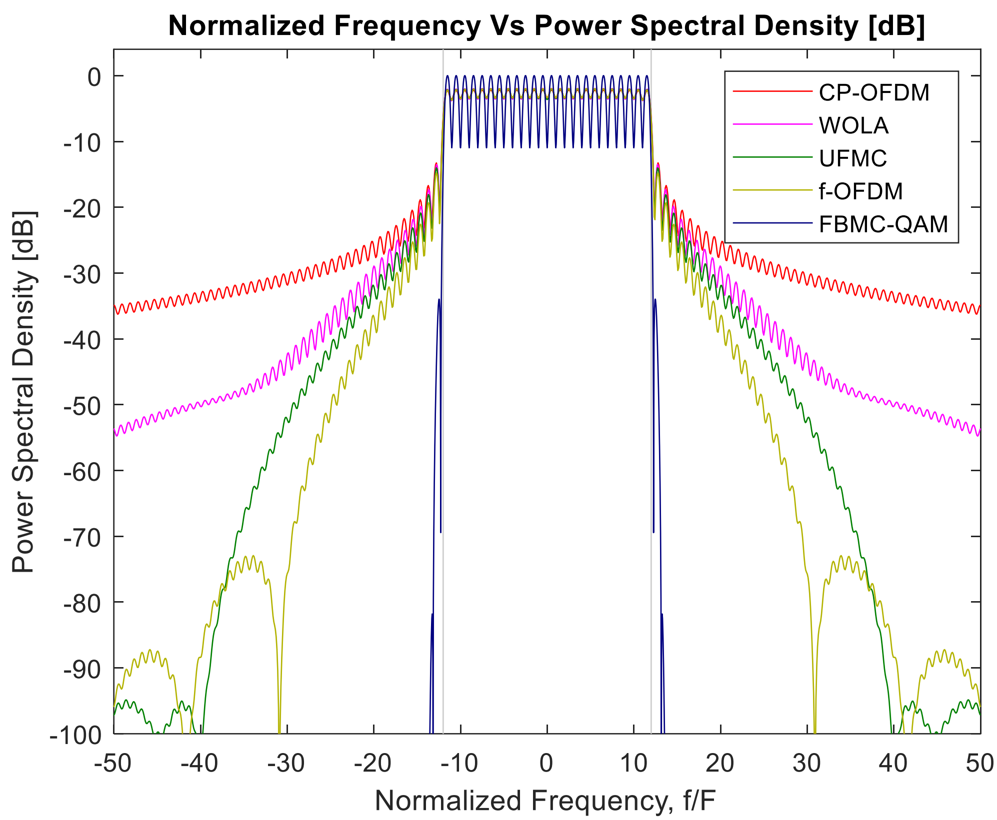

Figure 4.3 Comparison of Normalized Frequency Versus Power spectral density versus for FBMC

4.4 Comparison of Time-Frequency Efficiency versus Number of Subcarriers

Figure 4.4 compares the time-frequency efficiency (TF) versus number of subcarriers of FBMC-QAM with that of OFDM. The time frequency efficiency of FBMC has better performance on Time Frequency efficiency with a given subcarrier when compared to OFDM. Also increasing the number of subcarriers also increase the time frequency efficiency of both FBMC and OFDM systems. When using a small number of time-symbols, for example, K = 1 for f-OFDM and K = 2 for FBMC, f-OFDM exhibits better performance than FBMC. This is due to the larger guard time required in FBMC, assuming no overlapping between blocks is possible. However, when using approximately K = 5 complex time-symbols (K = 10 real-symbols), the time-frequency efficiency of FBMC becomes better than that of f-OFDM. This crossover point, though, is strongly dependent on the number of subcarriers used. Once the number of time-symbols approaches infinity, which is approximately true in many cases because blocks (sub-frames) can easily overlap, only OOB emissions are relevant and FBMC strongly outperforms f-OFDM.

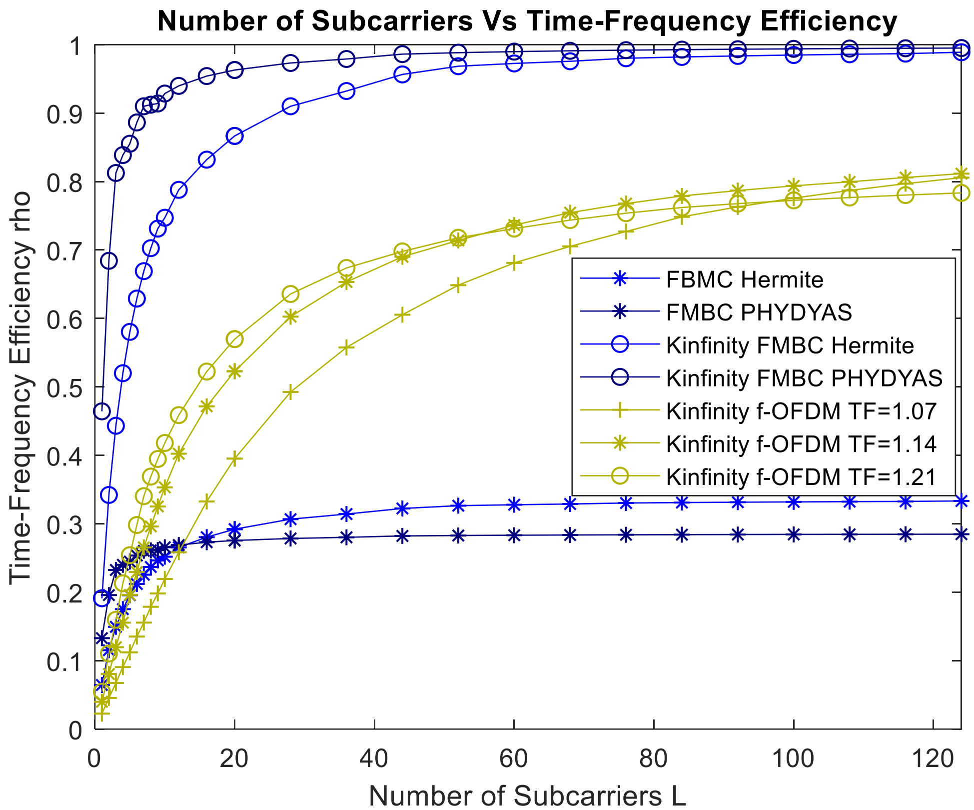

Figure 4.4 Time Frequency Efficiency (TF) of f-FBMC and OFDM

4.5 Comparison of SIR and Normalized Guard Band

Figure 4.5 shows how the SIR, depends on the normalized guard band. One can note that the higher the guard band, the less interference is observed. As illustrated in Figure, OFDM, WOLA, f-OFDM and UFMC experiences higher interference compared to FBMC. For instance, The interference is improved from 20.002dB (in OFDM) to 52.225 dB(FBMC) at a given guard band of 0.05 which shows a great improvement. Without receive windowing and filtering, the interference from user 1 to user 2 is higher than the interference from user 2 to user 1, as can be deduced from Figure 4.5. Once windowing and filtering are applied at the receiver, both users experience approximately the same interference power. Techniques like WOLA, UFMC, and f-OFDM can improve the signal-to-interference ratio (SIR), but their performance is still not as good as that of FBMC. Assuming an SIR of 45 dB is required, f-OFDM needs a guard band of FG = 0.24 FL. This results in a time-frequency efficiency for user 2 of $\rho = 1 / (1.24 \times 1.27) = 0.64$. In contrast, FBMC has a much higher efficiency of $\rho = 0.97$. Therefore, the data rate in FBMC is approximately 50% higher than in f-OFDM. One reason for this is the high subcarrier spacing in FBMC.

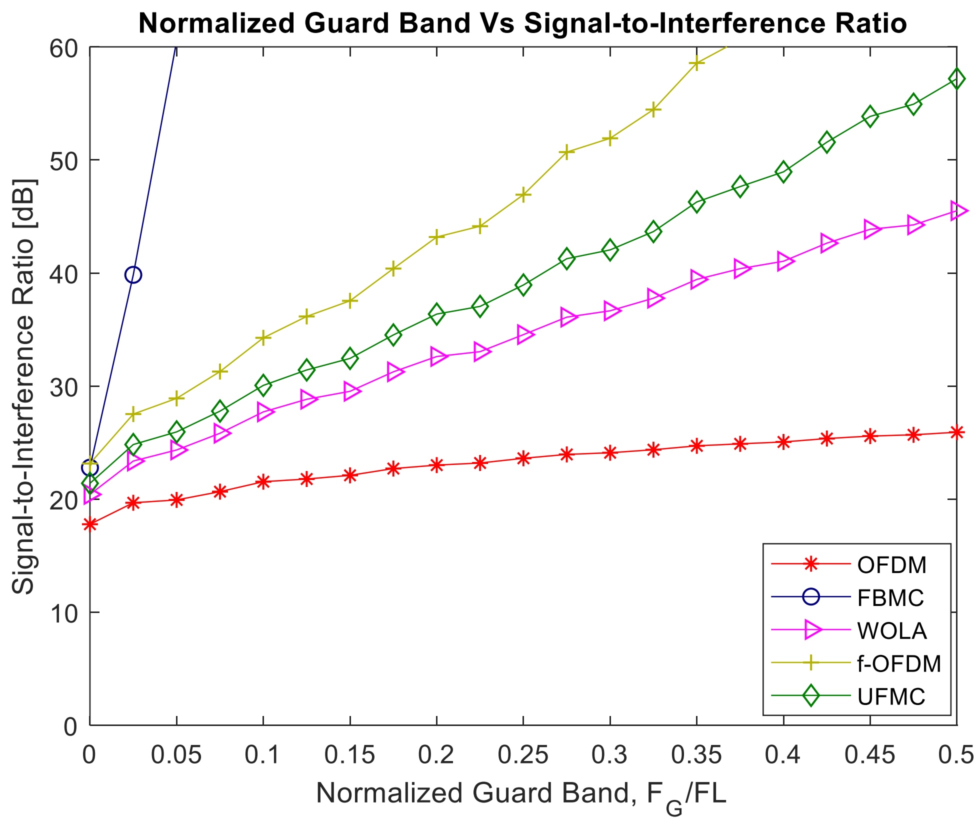

Figure 4.5 Comparison of Normalized Guard Band to Signal to Interference Ratio

4.6 BER comparison of FBMC, OFDM, UFMC , WOLA and f-OFDM

In order to support a large number of users' higher order, QAM is the best solution; however, the main drawback of using the higher order QAM system is complexity and it degrades the BER performance, which requires small values of BER (erroneous bit divided by total number of bits) in order to improve system performance. Bit error rate comparison is another performance metric to compare the performance of multicarrier modulation techniques in the communication system. The system with small number of BER has good performance than a system with higher number of BER. Figure 4.6 shows the BER performance of the FBMC system under different signal to noise ratios. The simulation is done for the Doubly selective flat fading channel model using the signal to noise ratio of -5 to 30 dB, QAM order of (64, 256, and 1024). The main aim of the simulation of this result is just to show the effect of higher order QAM on BER. The result shows that as QAM order increases, the FBMC system can support greater number of signals to noise ratio. However, the BER performance is not good compared to BER result of FBMC with lower order QAM. According to the simulation result, in order to improve the BER performance, the lower order QAM is preferable than the higher order QAM. However, lower QAM order cannot support the large signal to noise ratio and cannot support large number of users. To support massive communication in future, we are supposed to use higher order QAM. Figure 4.6 compares the bit error rate comparison of FBMC, OFDM, UFMC, WOLA and f-OFDM. We can see that the bit error rate has a slight improvement in FBMC in doubly selective fading channel compared to OFDM, filtering and windowing cases. This robustness makes FBMC preferred in doubly selective fading channel.

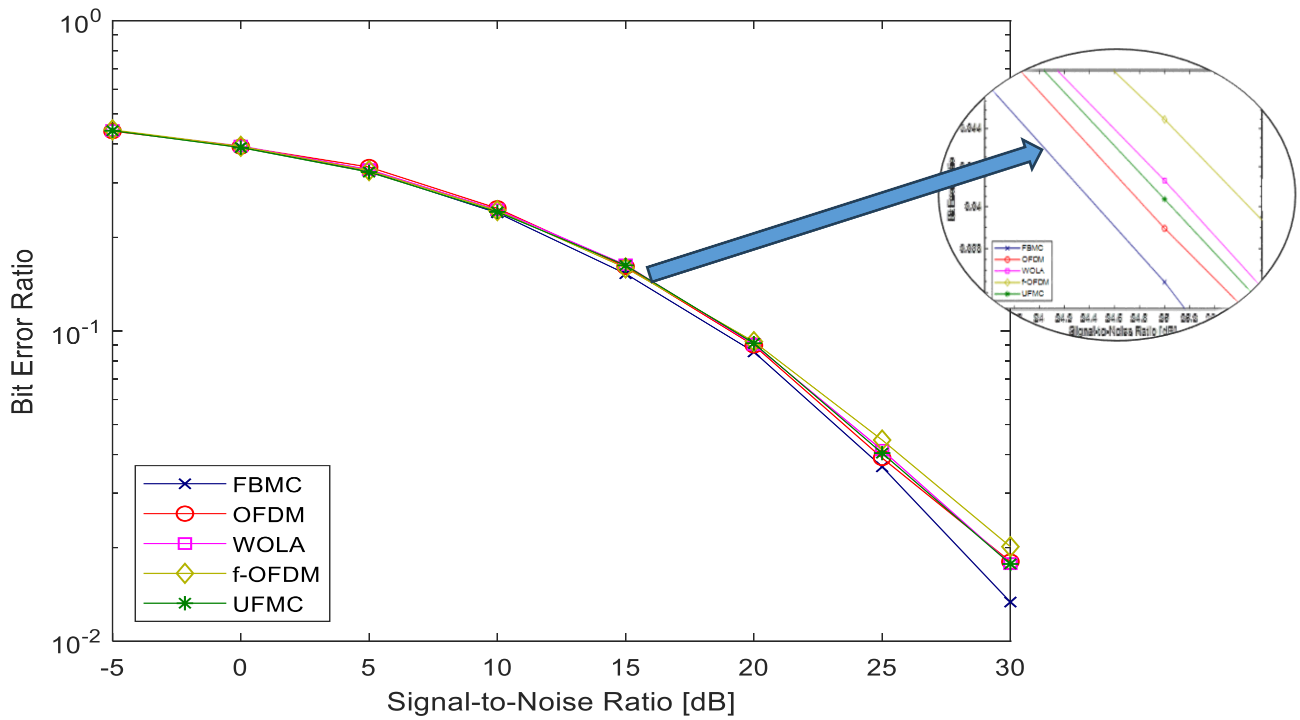

Figure 4.6 BER comparison of FBMC, OFDM, UFMC, WOLA and f-OFDM with 256QAM

4.7 Bit Error Rate Performance comparison in Slow Fading Environment

Figure 4.7 and 4.8 shows the bit error rate performance of OFDM, WOLA-OFDM, F-OFDM, UFMC, and FBMC/OQAM with slow fading environment. To simulate the slow fading environment Pedestrian channel selected and the performance of QAM 256 and 1024 compared.

One can note that the BER value of FBMC/QAM is least, which has technical meaning of better BER performance compared to other multicarrier modulation techniques. Thus error making possibility of FBMC/QAM is less compared to all other systems.

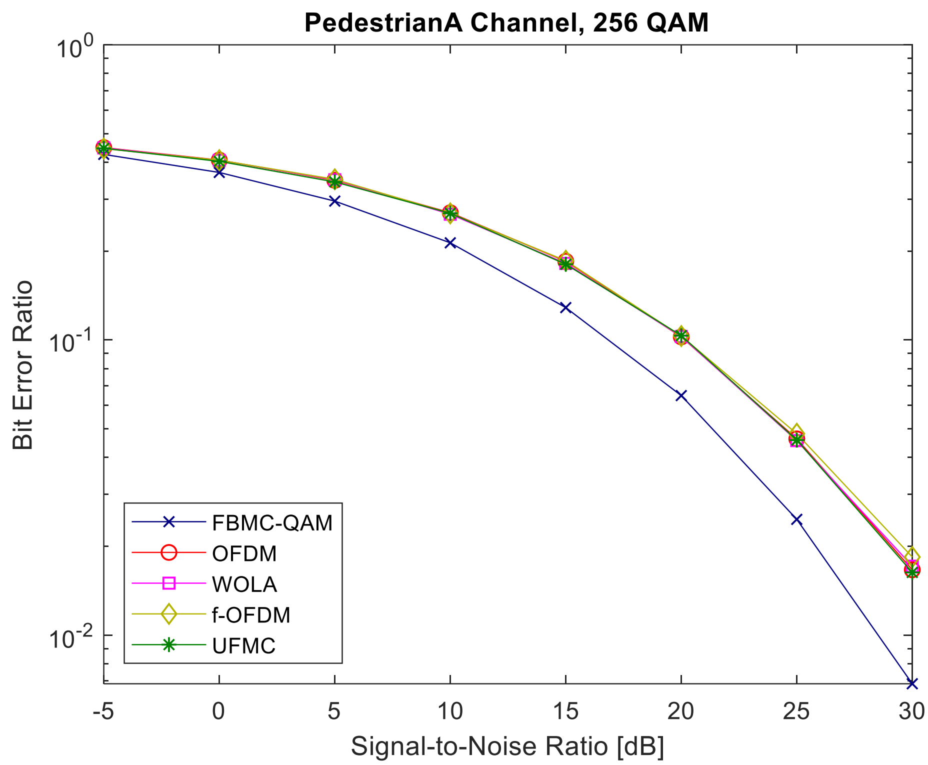

Figure 4.7 FBMC-QAM Pedestrian A Channel Performance/QAM-256/

As in the figure 4.7 depicted the FBMC-QAM outperform other multicarrier modulation tetchiness with the slow fading environment. Figure 4.8 shows that the performance evaluation of 1024 QAM in pedestrian channel. Its noted that the bit error rate is getting higher with order QAM.Moreover the effect of high order modulation/increasing modulation order assessed in the presence of slow fading. According to the simulation results, a lower order QAM is better than a higher order QAM for improving the BER performance. Lower QAM order, however, is unable to handle a high signal to noise ratio or a big user base. We are expected to deploy higher order QAM in the future to support large-scale communication.

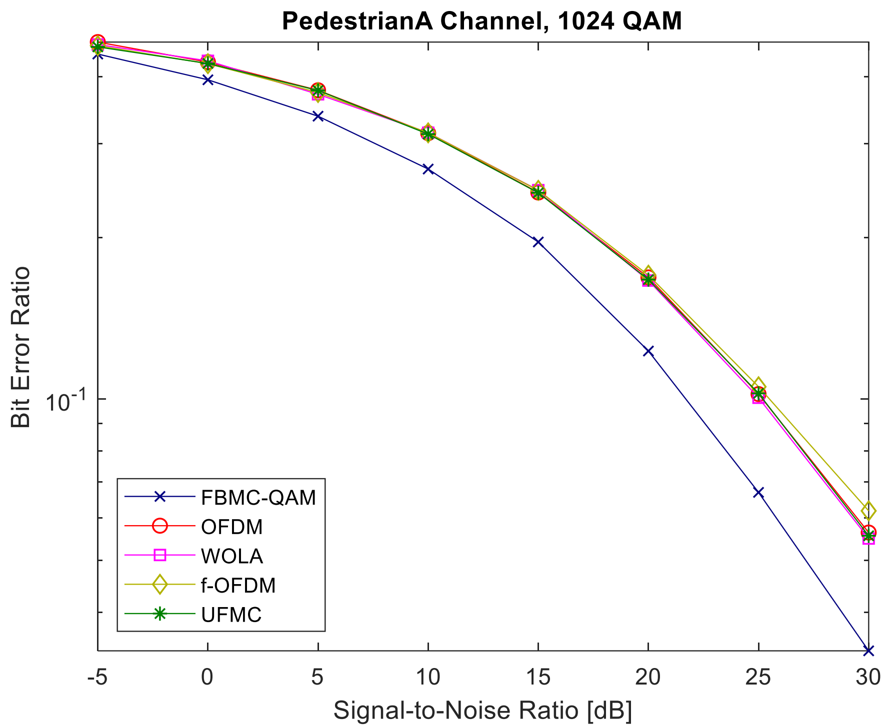

Figure 4.8 FBMC-QAM Pedestrian A Channel Performance 1024-QAM

4.8 Bit Error Rate Performance comparison in Fast Fading Environment

The bit error rate performance of several multicarrier modulation schemes for the vehicular channel model at 256 QAM and 1024 QAM, respectively, is displayed in Figures 4.9 and 4.10. The FBMC/QAM with Hermite filter has the lowest BER value across all numbers, making it the best system in comparison to all other systems that need to be improved. The FBMC/QAM has the lowest BER value across all figures, making it the best system to improve BER when compared to all other systems.

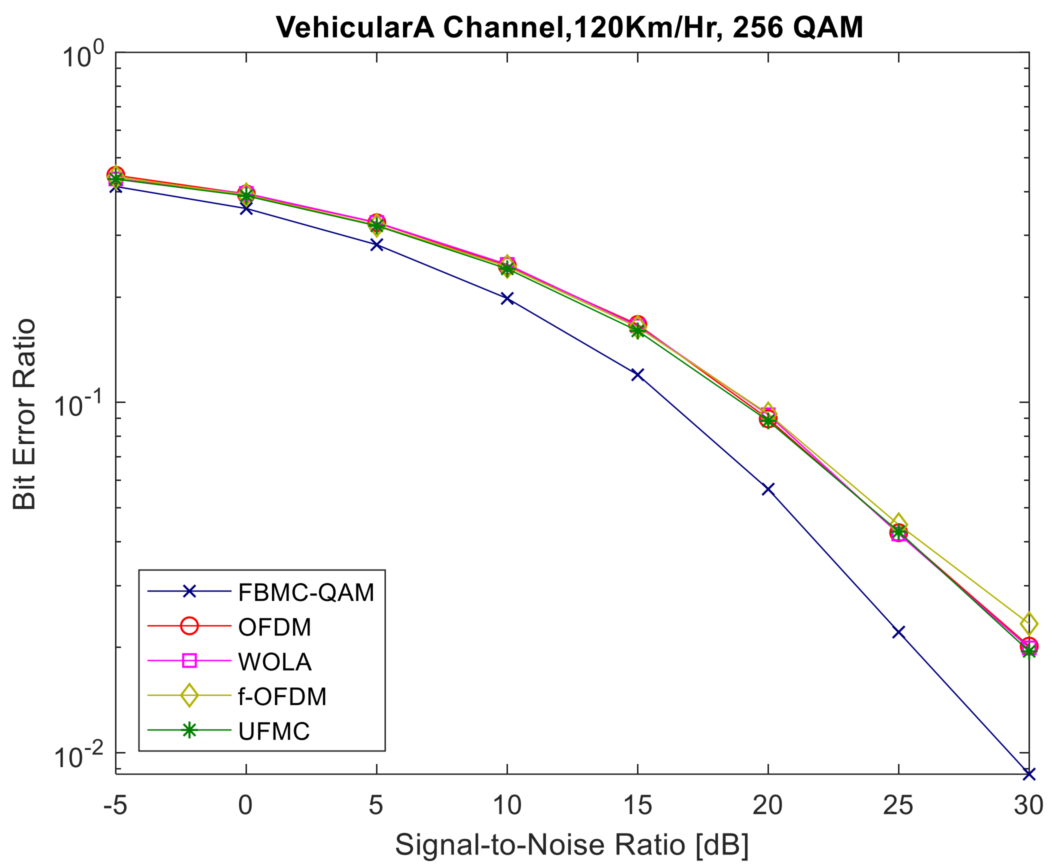

Figure 4.9 Vehicular Channel Model for 256-QAM

The performance of high order QAM/1024 QAM was also investigated/. Figure 4.10 shows that high order QAM increases the bit error rate but suitable for large data rate.

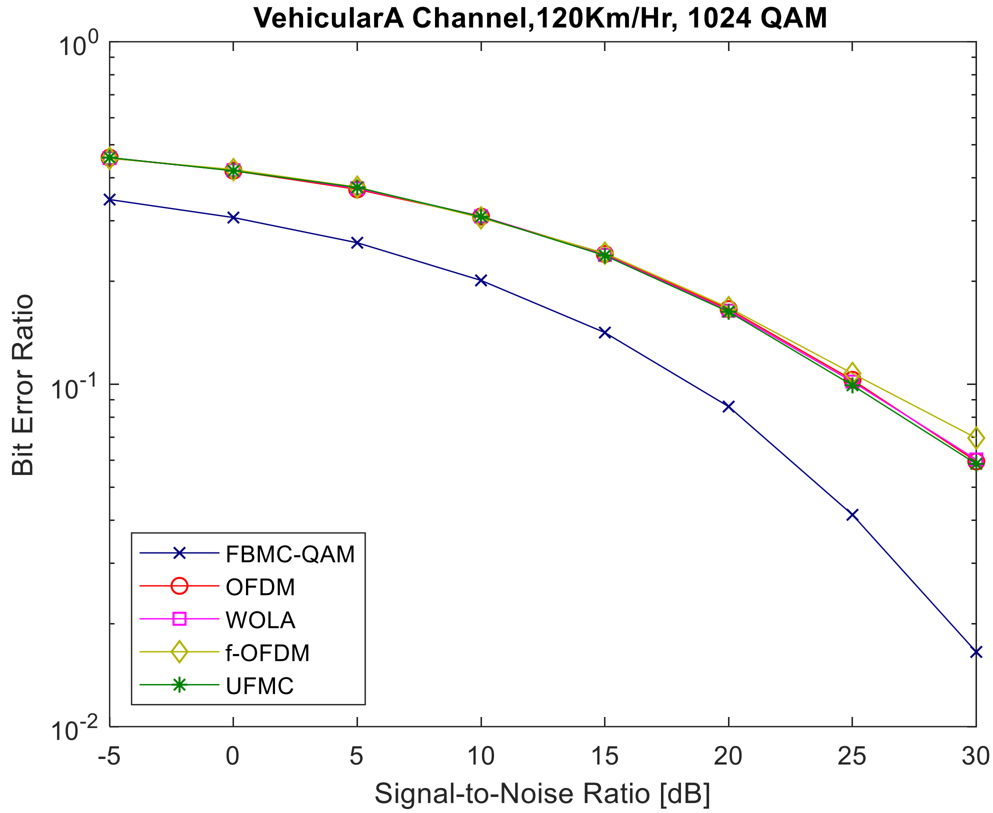

Figure 4.10 Vehicular Channel Model for 1024-QAM

To justify the performance increases numerically, the BER value of all system at modulation order 1026 at 10 dB is shown as follows: FBMC/QAM has BER value of $0.05 \times 10{-}0^{1}$, F-OFDM has BER value of 0.08×10^{-1} , WOLA-OFDM has BER value of 0.089×10^{-1} and UFMC has BER value of 0.0599×10^{-1} .

4.9 Performance Comparison of different Channel Estimation Techniques

Figure 4.11 depict the performance comparison of different channel estimation techniques in FBMC under doubly selective fading channel. Using the STA scheme outperforms other channel estimating techniques in terms of performance. As presented in Fig. 4.11, the TRFI scheme exhibits a modest performance gain over all traditional schemes when adopting high modulation order (64,256,1024QAM). This indicates that the TRFI scheme's frequency-domain interpolation is successful in predicting the channel at the erratic subcarriers. On the other hand, the classical STA scheme suffers from a severe degradation as noticed in Fig. below.

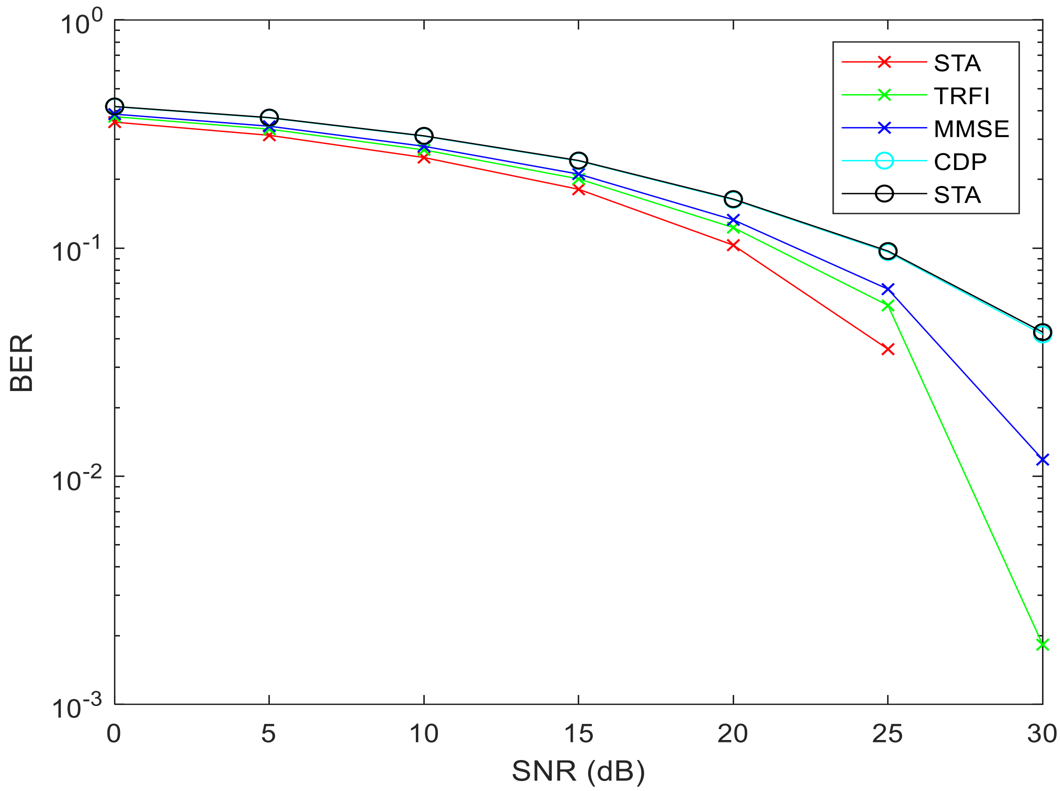

Figure 4.11 Comparison of channel estimation in FBMC

Table 4.2 Comparison of channel estimation in 64,256 and 1024 QAM

Modulation order	STA	TRFI	MMSE	CDP	STA
QAM 64	0.0766	0.0928	0.1028	0.1328	0.1338
QAM 256	0.0691	0.0902	0.1002	0.1310	0.1322
QAM 1024	0.0659	0.0877	0.802	0.1276	0.1301

4.10 Comparison of computational complexity of FBMC and OFDM

One of the major drawbacks of FBMC is its computational complexity. The computational complexity of FBMC and OFDM is compared in fig 4.12. Compared to traditional OFDM, FBMC has more computational complexity despite its many benefits. Any multicarrier scheme's computational complexity can be measured by counting the real multiplications needed to compute an output sequence with length N complex values. when the output sequence N has complex values. Both FBMC and OFDM get more difficult as the number of complex valued output sequences increases.

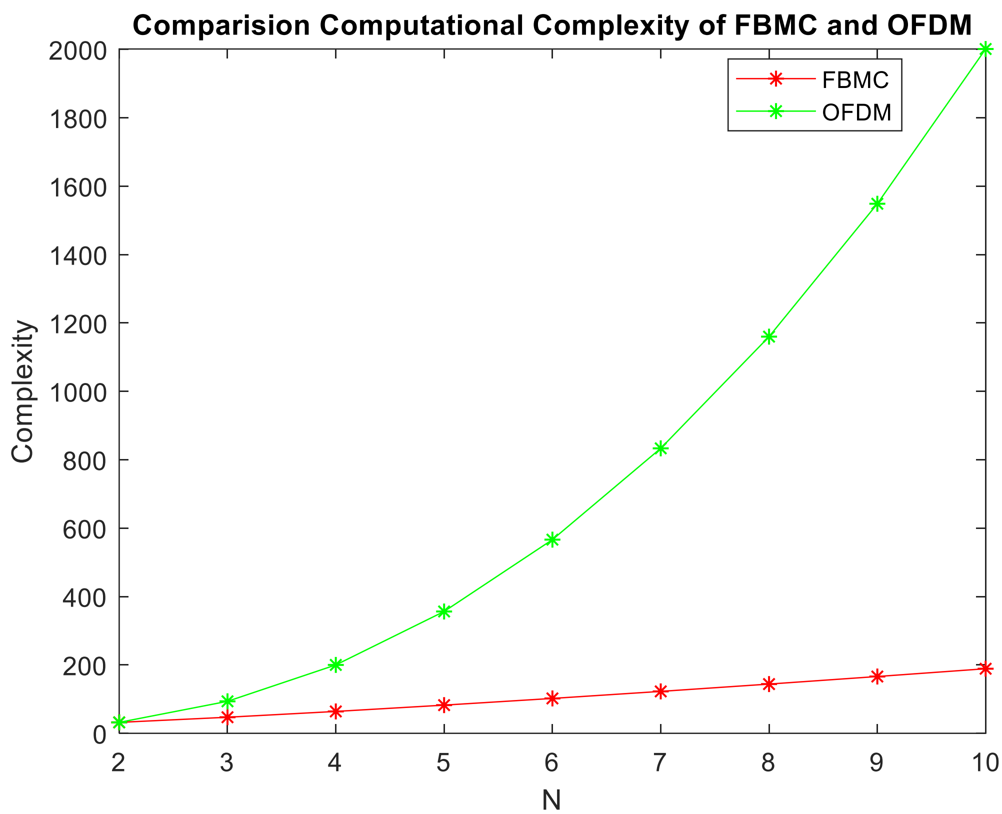

Figure 4.12 Computational complexity comparison of FBMC and OFDM

4.11 Comparison of Throughput of FBMC, UFMC, OFDM, f-OFDM and

Figure 4.13 shows the comparison of throughput of FBMC, UFMC, OFDM, f-OFDM and WOLA-OFDM. Because FBMC has no CP overhead and a higher usable bandwidth than OFDM, it can achieve a better throughput. With the same transmit power, both OFDM and FBMC have a 0.82 dB lower SNR than OFDM because the power is distributed over a wider bandwidth in FBMC. The throughput saturates, which is an important observation. The throughput improves by about 30% if the SNR is raised from 0 dB to 10 dB, or by a factor of 10. However, the throughput only improves by 20% if the SNR is raised from 20 dB to 30 dB, which is also a factor of 10. Consequently, a high SNR results in a minor throughput boost at the expense of much greater power and hardware expenditures.

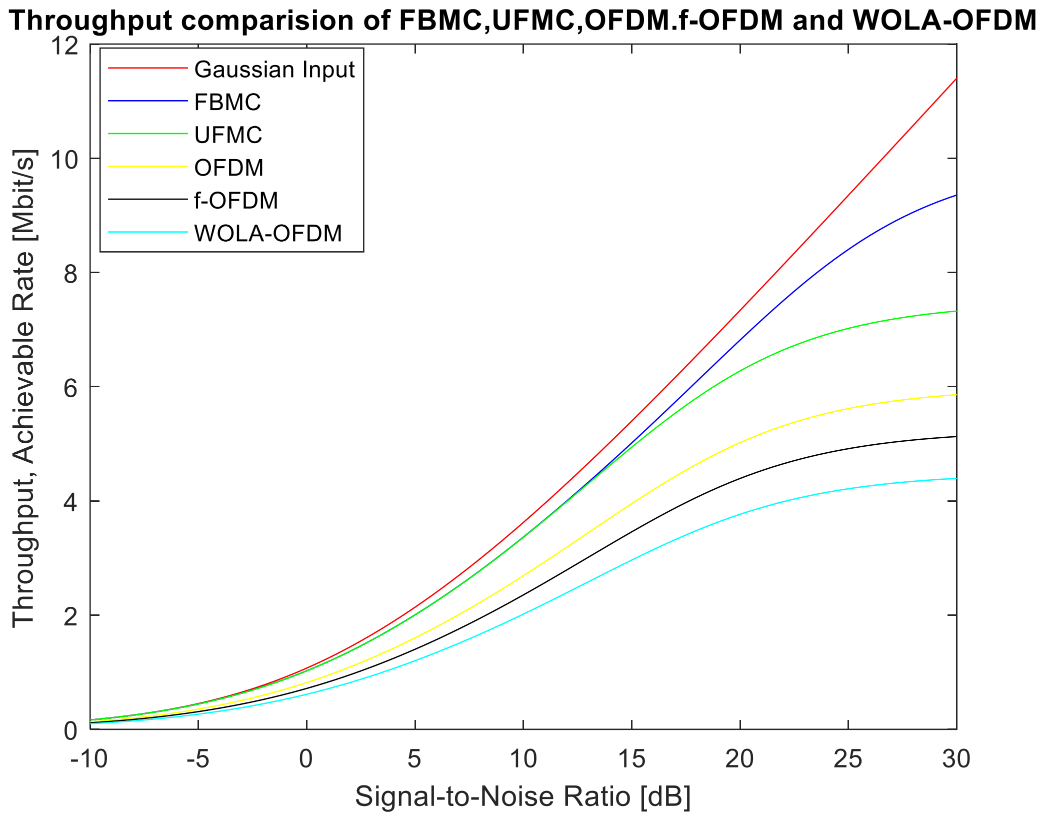

Figure 4.13 Throughput comparison of FBMC,UFMC, OFDM, f-OFDM and WOLA-OFDM

5. CONCLUSIONS AND RECOMMENDATIONS

5.1 Conclusions

In this thesis the performance of FBMC, UFMC, WOLA and f-OFDM investigate in doubly selective fading channel. The major drawback found in FBMC is that its computational complexity. Moreover, different the prototype filter was also compared and the outperforming filter was chosen for enhancing the performance of FBMC. Based on the simulation results, the following conclusion can be drawn.

Based on the simulation results, the following conclusion can be drawn.

- Power Spectral density decay rate of Hermite prototype filter is better/faster/ than PHYDYAS filter and provides less OOB emission.
- The overlapping factor has a great contribution on the side lobe energy. Increased overlapping factor provides decays faster of OOB emission.
- FBMC-QAM is more spectrally efficient and has much improved spectral properties and low BER.
- OFDM, WOLA, f-OFDM and UFMC experiences higher interference compared to FBMC at a given guard band.
- As QAM order increases, the FBMC system can support greater number of signals to noise ratio. However, the BER performance is not good compared to BER result of FBMC with lower order QAM.
- FBMC provided larger throughput compared to OFDM.

5.2 RECOMMENDATION AND FUTURE WORKS

In this thesis the performance of FBMC with high order QAM in doubly selective fading channel was examined. The following issues are the future scope of this thesis.

- To reduce the computational complexity of the FBMC System by deploying channel equalizer and compare with conventional FBMC System.
- To study the capacity improvement of FBMC transmission in the context of massive MIMO by considering single-tap-per-subcarrier equalization using the conventional linear combiners such as MRC, ZF and MMSE.

Research Fund Acknowledgement

This research project is funded by Adama Science and Technology University under the grant number ASTU/SM-R/1025/24, Adama, Ethiopia.

REFERENCES

A. Viholainen, M. Bellanger, and M. H. (n.d.). Prototype filter and structure optimization. *Website: Www.Ict-Phydyas.Org, Document D*, 22.

A. Viholainen, T. Ihalainen, T. Hidalgo Stitz, M. Renfors, and M. B. (2009). Prototype filter design for filter bank based multicarrier transmission, in August 2009, pp. 1359-1363. *European Signal Processing Conference (EUSIPCO 2009), 17th*, 1359–1363.

Abbas, A. K., Jamel, T. M., & Nahar, A. K. (2023). An overview for filter bank multicarrier using channel estimation 5G wireless communication. *AIP Conference Proceedings*, *2820*. https://doi.org/10.1063/5.0150798

Abboud, M. K., & Sabbar, B. M. (2020). Performance evaluation of high mobility OFDM channel estimation techniques. *International Journal of Electrical and Computer Engineering*, *10*(3), 2562–2568. https://doi.org/10.11591/ijece.v10i3.pp2562-2568

Abouldahab, M. A., Fouad, M. M., & Roshdy, R. A. (2018). A proposed preamble based channel estimation method for FBMC in 5G wireless channels. *National Radio Science Conference, NRSC, Proceedings*, *2018-March*(Nrsc), 140–148. https://doi.org/10.1109/NRSC.2018.8354382

Alhava, J., & Renfors, M. (n.d.). *Exponentially-modulated filter bank-based transmultiplexer*. 233–236.

Andrews, J. G., Buzzi, S., Choi, W., Hanly, S. V., Lozano, A., Soong, A. C. K., & Zhang, J. C. (2014). What will 5G be? *IEEE Journal on Selected Areas in Communications*, *32*(6), 1065–1082. https://doi.org/10.1109/JSAC.2014.2328098

Bellanger, M. G. (2001). Specification and design of a prototype filter for filter bank based multicarrier transmission. *ICASSP, IEEE International Conference on Acoustics, Speech and Signal Processing - Proceedings*, *4*, 2417–2420. https://doi.org/10.1109/icassp.2001.940488

Bendimerad, M. Y., Senhadji, S., & Bendimerad, F. T. (2021). *Prototype Filters and Filtered Waveforms for Radio Air-Interfaces: A Review*. 1–26. http://arxiv.org/abs/2104.01373

C.Daniel, Arajo, Taras Maksymyuk, Andr L. F. de Almeida1, Tarcisio Ma ciel1, Joo C. M. Mota1, and M. J. (n.d.). Massive MIMO: Survey and Future Research Topics” , Communication Systems. *Evolution and the Revolution of 5G Wireless*.

Chen-Hu, K., Estrada-Jiménez, J. C., García, M. J. F. G., & Armada, A. G. (2017).

Superimposed training for channel estimation in FBMC-OQAM. *IEEE Vehicular Technology Conference*, *2017-Septe*, 1–5. https://doi.org/10.1109/VTCFall.2017.8287938

D. S. Waldhauser, L. G. Baltar, and J. A. N. (n.d.). MMSE subcarrier equalization for filter bank based multicarrier systems,. *In IEEE Workshop on Signal Processing Advances in Wireless Communications, 2008*.

Dumari, H. T., Gelmecha, D. J., Shakya, R. K., & Singh, R. S. (2023). *BER and PSD Improvement of FBMC with Higher Order QAM Using Hermite Filter for 5G Wireless Communication and beyond*. *2023*.

Gizzini, A. K., Chafii, M., Nimr, A., & Fettweis, G. (2020). Joint TRFI and Deep Learning for Vehicular Channel Estimation. *2020 IEEE Globecom Workshops, GC Wkshps 2020 - Proceedings*, 1–6. https://doi.org/10.1109/GCWkshps50303.2020.9367412

He, Z., Zhou, L., Yang, Y., Chen, Y., Ling, X., & Liu, C. (2019). Compressive Sensing-Based Channel Estimation for FBMC-OQAM System under Doubly SeHe, Z., Zhou, L., Yang, Y., Chen, Y., Ling, X., & Liu, C. (2019). Compressive Sensing-Based Channel Estimation for FBMC-OQAM System under Doubly Selective Channels. IEEE Acce. *IEEE Access*, *7*(c), 51150–51158. https://doi.org/10.1109/ACCESS.2019.2898896

Hosseiny, H., Farhang, A., & Farhang-Boroujeny, B. (2020). Spectrally Efficient Pilot Structure and Channel Estimation for Multiuser FBMC Systems. *IEEE International Conference on Communications*, *2020-June*. https://doi.org/10.1109/ICC40277.2020.9148851

Hussein, W., Audah, K., Noordin, N. K., Kraiem, H., Flah, A., Fadlee, M., & Ismail, A. (2023). Least Square Estimation-Based Different Fast Fading Channel Models in MIMO-OFDM Systems. *International Transactions on Electrical Energy Systems*, *2023*. https://doi.org/10.1155/2023/5547634

I. Goodfellow, Y. Bengio, and A. C. (2016). Deep Learning. *MIT Press, http://www.deeplearningbook.org.*

J. A. Fernandez, K. Borries, L. Cheng, B. V. K. Vijaya Kumar, D. D. Stan cil, and F. B. (2012). Performance of the 802.11p Physical Layer in Vehicle_to-Vehicle Environments. *IEEE Transactions on Vehicular Technology*, *61*(1), 3–14.

Kamurthi, R. T., & Chopra, S. R. (2018). Review of UFMC technique in 5G. *Proceedings - 2nd International Conference on Intelligent Circuits and Systems, ICICS 2018*, *April*

2018, 121–125. https://doi.org/10.1109/ICICS.2018.00034

Kassaw, F. T. and C. A. (2019). *Comparative performance analysis of modulation formats for 5g wireless system*. *Addis Ababa Institute of Technology*, *Addis Ababa*, *Ethiopia*.

Kim, C., Yun, Y. H., Kim, K., & Seol, J. Y. (2016). Introduction to QAM-FBMC: From Waveform Optimization to System Design. *IEEE Communications Magazine*, *54*(11), 66–73. https://doi.org/10.1109/MCOM.2016.1600384CM

Kishore, K. K., Umar, P. R., & Naveen, V. J. (2017). Comprehensive Analysis of UFMC with OFDM and FBMC. *Indian Journal of Science and Technology*, *10*(17), 1–7. https://doi.org/10.17485/ijst/2017/v10i17/114337

Kundrapu, S., Dutt, S. I., Koilada, N. K., & Raavi, A. C. (2019). Characteristic Analysis of OFDM, FBMC and UFMC Modulation Schemes for Next Generation Wireless Communication Network Systems. *Proceedings of the 3rd International Conference on Electronics and Communication and Aerospace Technology, ICECA 2019*, 715–721. https://doi.org/10.1109/ICECA.2019.8821991

L. Marijanovic, S. Schwarz, and M. R. (n.d.). MMSE equalization for FBMC transmission over doubly-selective channels. *" In Thirteenth International Symposium on Wireless Communication Systems, (Poznan, Poland),* 1–6.

Louveaux, A. I. and J. (2009). Per subchannel equalization for MIMO FBMC/OQAM systems. *In IEEE Pacific Rim Conference on Communications, Computers*.

Marian Joseph Jeffery, J., Masapalli, L., Nookala, V. M., Dasari, S. P., & Kirthiga, S. (2020). Peak to Average Power Ratio and Bit Error Rate Analysis of MultiCarrier Modulation Techniques. *Proceedings of the 2020 IEEE International Conference on Communication and Signal Processing, ICCSP 2020,* 1443–1446. https://doi.org/10.1109/ICCSP48568.2020.9182172

Matz, G., Schafhuber, D., Gröchenig, K., Hartmann, M., & Hlawatsch, F. (2007). Analysis, optimization, and implementation of low-interference wireless multicarrier systems. *IEEE Transactions on Wireless Communications*, *6*(5), 1921–1930. https://doi.org/10.1109/TWC.2007.360393

Nam, H., Choi, M., Han, S., Kim, C., Choi, S., & Hong, D. (2016). A New Filter-Bank Multicarrier System with Two Prototype Filters for QAM Symbols Transmission and Reception. *IEEE Transactions on Wireless Communications*, *15*(9), 5998–6009.

https://doi.org/10.1109/TWC.2016.2575839

Nissel, R. (2016). Symbol detection in high speed channels. *In The Vienna LTE-Advanced Simulators: Up and Downlink, Link and System Level Simulation, Singapore:*, 39–60,.

Nissel, R., Ademaj, F., & Rupp, M. (2018). Doubly-Selective Channel Estimation in FBMC-OQAM and OFDM Systems. *IEEE Vehicular Technology Conference*, *2018-Augus*(3), 1–5. https://doi.org/10.1109/VTCFall.2018.8690864

Nissel, R., & Rupp, M. (2017). OFDM and FBMC-OQAM in Doubly-Selective Channels: Calculating the Bit Error Probability. *IEEE Communications Letters*, *21*(6), 1297–1300. https://doi.org/10.1109/LCOMM.2017.2677941

Pranathi, K., & Naveena, A. (2023). *Estimation of Doubly Selective Channel in FBMC-OQAM and OFDM Systems* (Issue Mcm). Springer Nature Singapore. https://doi.org/10.1007/978-981-99-1588-0_14

Ramadhan, A. J. (2019). Implementation of a 5G filtered-OFDM waveform candidate. *International Journal of Engineering Research and Technology*, *12*(4), 500–507.

Sahin, A., Guvenc, I., & Arslan, H. (2014). A survey on multicarrier communications: Prototype filters, lattice structures, and implementation aspects. *IEEE Communications Surveys and Tutorials*, *16*(3), 1312–1338. https://doi.org/10.1109/SURV.2013.121213.00263

Signal, R. research in, & Processing. (2009). P. Vandewalle, J. Kovacevic, and M. Vetterli. *IEEE Signal Processing Magazine*, *26,no*.

Sim, D., & Lee, C. (2019). Performance Evaluation Based on Effective Channel Analysis for FBMC-QAM System with Two Prototype Filters. *IEEE Transactions on Communications*, *67*(5), 3552–3565. https://doi.org/10.1109/TCOMM.2019.2893316

Vaidyanathan, P. P. (1993). Multirate Systems and Filter Banks. *Prentice Hall*.

Vaigandla, K. K., Siluveru, M., & Karne, R. (2023). Study and Comparative Analysis of OFDM and UFMC Modulation Schemes. *Journal of Electronics,Computer Networking and Applied Mathematics*, *32*, 41–50. https://doi.org/10.55529/jecnam.32.41.50

Wang, Y., Guo, Q., Xiang, J., & Liu, Y. (2023). Doubly selective channel estimation and equalization based on ICI/ISI mitigation for OQAM-FBMC systems. *Physical Communication*, *59*, 102120. https://doi.org/10.1016/j.phycom.2023.102120

X. Zhang, M. Jia, L. Chen, J. Ma, and J. Q. (2015). Filtered-OFDM-enabler for flexible waveform in the 5th generation cellular networks. *In IEEE Global Communications Conference (GLOBECOM)*, 1–6.

Yun, Y. H., Kim, C., Kim, K., Ho, Z., Lee, B., & Seol, J. Y. (2015). A new waveform enabling enhanced QAM-FBMC systems. *IEEE Workshop on Signal Processing Advances in Wireless Communications, SPAWC*, *2015-Augus*, 116–120. https://doi.org/10.1109/SPAWC.2015.7227011

Z. Zhao, X. Cheng, M. Wen, B. Jiao, and C. W. (2013). Channel Estimation Schemes for IEEE 802.11p Standard. *IEEE Intelligent Transportation Systems Magazine*, *5*(4), 38–49.

Zayani, R., Medjahdi, Y., Shaïek, H., & Roviras, D. (2016). WOLA-OFDM: A potential candidate for asynchronous 5G. *2016 IEEE Globecom Workshops, GC Wkshps 2016 - Proceedings*, *December*. https://doi.org/10.1109/GLOCOMW.2016.7849087

Zhang, X., Jia, M., Chen, L., Ma, J., & Qiu, J. (2015). Filtered-OFDM - Enabler for flexible waveform in the 5th generation cellular networks. *Proceedings - IEEE Global Communications Conference, GLOBECOM*. https://doi.org/10.1109/GLOCOM.2014.7417854

Zimmermann, G. (1998). Gabor Analysis and Algorithms. In *Gabor Analysis and Algorithms* (Issue June 2014). https://doi.org/10.1007/978-1-4612-2016-9